DYNAMIC CHARACTERISTICS OF GAS-SOLIDS FLUIDIZED BEDS USING RADIOACTIVE ISOTOPE TECHNIQUES

by

JOE JACKSON STEWART

B. S., Purdue University, 1959

A THESIS

submitted in partial fulfillment of the

requirements for the degree

MASTER OF SCIENCE

Department of Nuclear Engineering

KANSAS STATE UNIVERSITY
OF AGRICULTURE AND APPLIED SCIENCE

1961

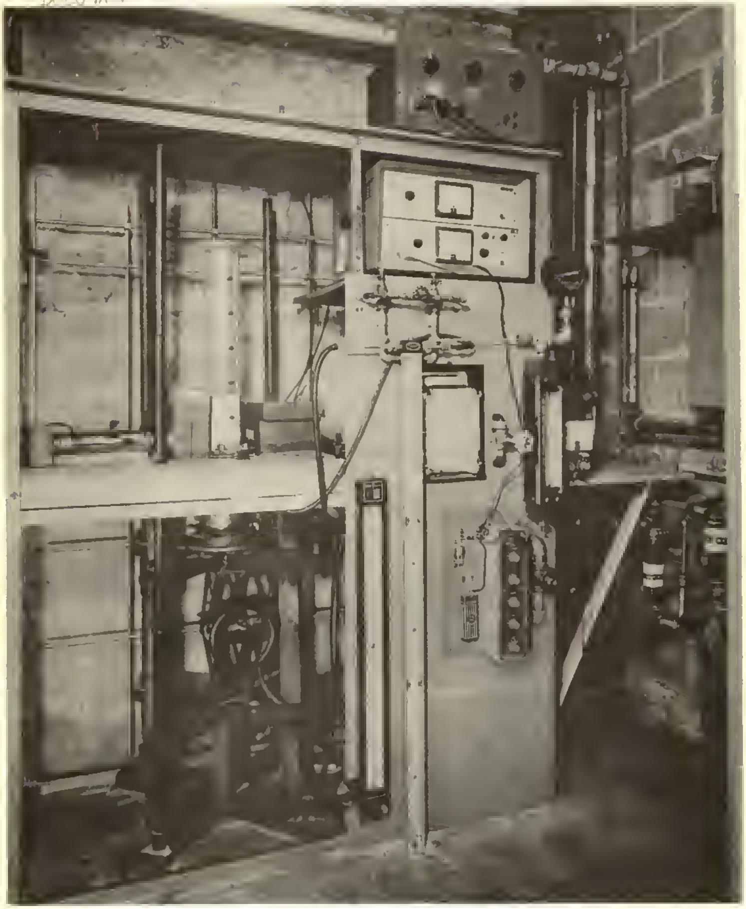

DYNAMIC CHARACTERISTICS OF GAS-SOLIDS FLUIDIZED BEDS
USING RADIOACTIVE ISOTOPE TECHNIQUES

By JOE JACKSON STEWART

Department of Nuclear Engineering—Kansas State University, Manhattan
Engineering Experiment Station, Project Number 284

TABLE OF CONTENTS

TABLE OF CONTENTS (cont.)

INTRODUCTION

Background

In the past twenty years the concept of fluidization and the fluidized bed has been utilized in many industrial processes. The reason for the increased activity in this field undoubtedly lies in the many advantages that the fluidized bed has over the fixed bed in certain industrial processes. Leva (6) and Othmer (9) have enumerated many of the advantages and disadvantages of fluidization. The most important of these are as follows:

Advantages

1. Agitation as a result of fluidization provides a more uniform temperature and solids distribution.

2. The smaller particle size of fluidized systems provides less resistance to diffusion through the particle. This is important in certain chemical reactions.

3. Fluidization permits a continuous addition and withdrawal of solids from the bed. This is important in refueling operations.

4. Heat transfer coefficients from the bed to the surroundings are higher for fluidized beds with comparable flow rates.

5. High solids-gas heat transfer rates are prevalent.

6. In many cases the pressure drop across the bed is less for a fluidized bed.

Dieadvantages

1. In general, concurrent flow ie found in fluidized bede. Thie is unfavorable to the driving force of the chemioal reactione.

2. Collisione between ths partioles may reeult in attrition of ths partiolee.

3. Erosion of the reaotor vsesel may ocour.

4. Ths fluid velooity muet be cloesly ooordinated with the properties of the particles. Thie rsstricts the vslocity range.

5. Fluidization with gae ie only possibls whsn ths reaction forms no liquid or wax. This rsstricts certain hydrocarbon eynthesie.

Some of ths more important applications of fluidization are ae follows: catalytio oracking of petroleum, oatalytio reforming, ooking, catalytio oxidation of ethylene, production of alkyl chlorides, iron-ors reduction, roaeting of pyritic orse, gold oree, and limsstone, sizing and drying, ooal gasification and oarbonization, hydrocarbon eyntheeis, production of phthalio anhydride, coating, airslide conveyore, aerosol filtration, nuclear reactore, reduction and fluorination of uranium, retorting of oil ehales, tsxtils drying, and smoking of tobaoco.

Ths Bubbls Phsnomsna

In epite of the fact that fluidized gas-eolide prooeesse have operated suocoeesfully, sevsral of the fundamental principles involved in the gas-flow msohaniem within a fluidized bed are relatively unexplored. It has been suggested and is generally accepted that there exists a two-phase system in the gas-solids fluidized bed. These two phases are known as the dense phase and the bubble phase. The dense phase consists of the solid particles and a portion of the gas held in the interstices of the solids, while the bubble phase represents totally gaseous matter. The effect is thus one of gas by-passing the dense phase in the form of bubbles. This means that only a portion of the total gas throughput comes into contact with the solids. This is very undesirable in many processes because it defeats one of the primary purposes of fluidization, to increase solids-gas contact. This lowers the efficiency of the process.

In addition, previous investigations have shown that the bubble phase passes through the bed at a velocity several times the superficial (gas velocity in empty column) gas velocity (1), (14). This factor also contributes an undesirable effect in that the two types of gas are held in the reactor different lengths of time. This leads to different degrees of conversion for the two phases.

These uncertainties involved in the bubble phenomena have emphasized the importance of the bubble formation in the fluidized bed.

Application to Nuclear Reactors

One of the most unique applications of fluidization that has been proposed is the fluid-bed nuclear reactor (14). The use of a fluid-bed core has the distinct advantage of comparative ease in addition of fresh fuel and in the withdrawal of spent fuel. Other advantages include freedom in control rod arrangement and favorable heat transfer characteristics.

The Texaco Development Corporation (14) has designed a gas-fluidized bed nuclear reactor. In this design uranium oxide or uranium carbide can be used as a fuel and hydrogen or helium as the fluidizing gas.

The Westinghouse Electric Corporation (14) has recently proposed an organic-moderated, fluidized-bed reactor using 1/8-inch-diameter uranium oxide pellets and a liquid organic coolant-moderator. The organic fluid would flow upward through the bed of uranium oxide pellets. Control would be achieved by regulating the bed expansion with the flow rate of organic coolant.

In nuclear reactors the uniformity of fluidization is quite important, and probably essential. The result of bubble formation would be the development of hot spots and thermal stresses when the coolant gas by-passed the solids. In addition, other uncertainties accompanying bubble formation could have undesirable effects upon the control of the reactor by bed expansion and/or contraction.

Purpose

Although a few research workers have made studies of bubble formation in gas-solids fluidized beds, there still exists an area of uncertainty which should be explained. Even though it is widely accepted that gas by-passing is characteristic of gas-solids fluidized systems, it would be desirable to minimize the effect of this inherent property.

Dotson (2), using the capacitance probe method in a statistically designed experiment, found that the most important variables affecting density fluctuations were gas velocity, height in bed, and particle size.

Morse and Ballou (8), Shuster and Kisliak (12), Dotson (2) and Romero (11) have all defined a type of uniformity or quality index in order to investigate the bubble effect. Baumgarten (1) did not present a quality index as such, but presented data on size and frequency of bubbles as a function of distance from the distributor for several operating variables. A more detailed description of these investigations will be discussed later. In each of these cases relatively little has been done with the defined index as a function of the operating variables and bed characteristics. It was the purpose of this investigation to introduce a statistical approach in defining an index of stability and uniformity, and in addition, to investigate the effect of gas velocity, height in bed, particle size, and packed bed height upon this index.

EXPERIMENTAL

General Consideration

Density fluctuations in the two-phase, gas-solids, fluidized bed were determined using the radiation attenuation method described by Petrick and Swanson (10), and Groshe (4). A radioactive γ-ray source provided a beam of γ-radiation which was directed through the center of the fluidizing column. Density fluctuations were determined by detecting, measuring, and recording the portion of γ-radiation which was not attenuated, the relation between density and attenuation being,

$$I/I_o = e^{-\mu d}$$

where I/I_o is the fraction of photons remaining in the beam after passage through an absorber of thickness d. The linear absorption coefficient, μ, is given by

$$\mu = (N_a/M)\,\sigma_T\,\rho$$

where N_a is Avagadro's number, M is the gram-atomic weight, ρ is the density of the absorbing medium, and σ_T is the microscopic cross section.

Dry air was used as the fluidizing medium, while spherical glass beads were used in the bed. The glass beads were of two sizes, 40-45 mesh and 80-100 mesh.

The variables, superficial air velocity, height in bed, particle size, and packed bed height, were investigated. Three air velocities were used; 30, 60, and 90 ft./min. Nine particle mixtures ranging from 100 percent 40-45 mesh to 100 percent 80-100 mesh, and packed bed heights of 3, 6, and 9 inches were investigated on the 100 percent particle mixtures. Complete vertical traverses of the fluidized bed were made in each case.

A detailed description of the experimental portion of this investigation follows.

Apparatus

A photograph of the equipment is shown in Fig. 1 while a schematic diagram is presented in Fig. 2. The equipment may be divided into two categories; (1), the column and its accessories, and (2), the gamma-ray source and nuclear instrumentation for detection, measurement, and recording of the transmitted gamma-ray beam.

<u>The Column and Its Accessories</u>. A 24-inch-high, 3.97-inch-diameter, lucite column was used. The column was covered at the top with a fine screen to permit the exhaust of the fluidizing air, but to retain any particles that might have been fluidized as high as the top of the column. The lower flange of the column was equipped with a pressure tap for measuring the pressure drop over the bed. Other taps were located every four inches up the column; however, none of these were used in this work. The lower flange of the column was bolted directly to the distributor

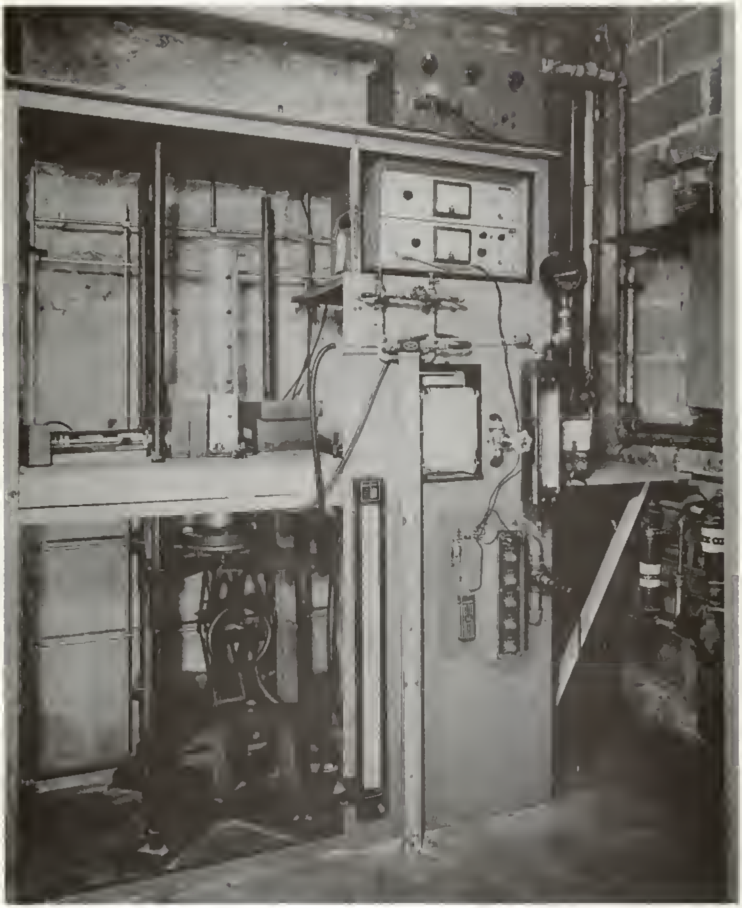

Fig. 1. Photograph of column and associated equipment.

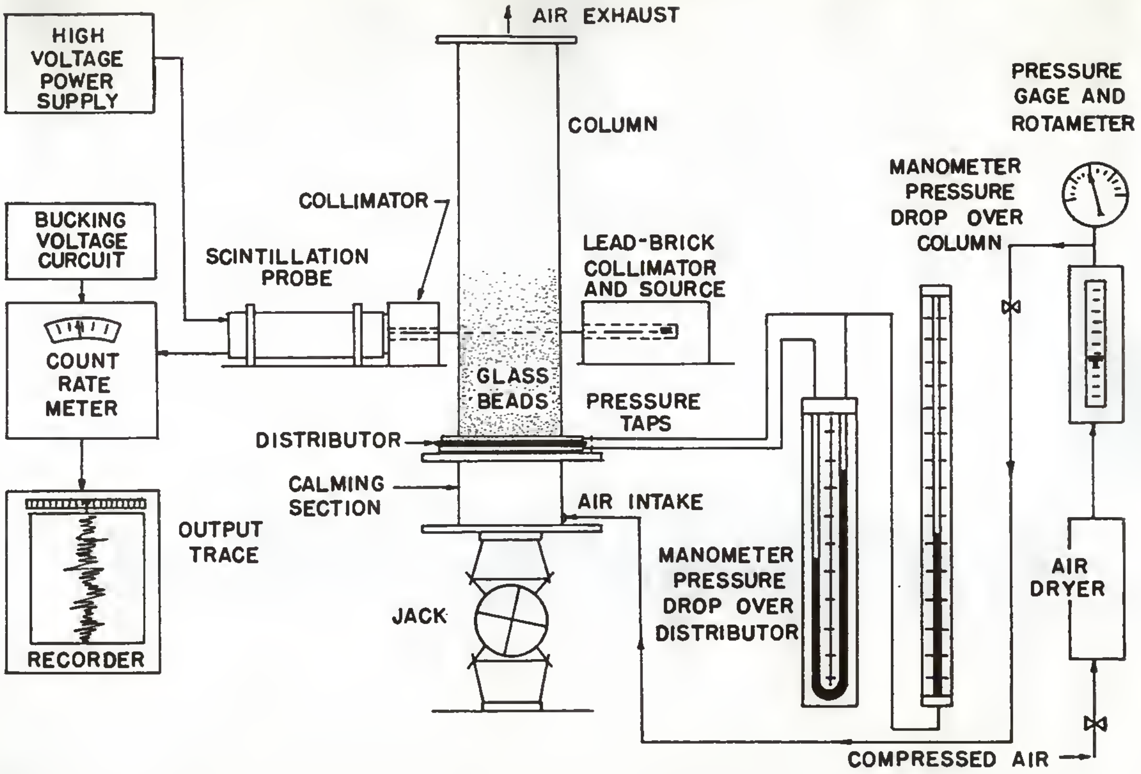

Fig. 2. Schematic diagram of column, accessories, and instrumentation.

assembly.

Accessories to the column included the distributor assembly for distributing the air, manometers for measuring the pressure drops over the column and across the distributor, an air supply to provide dry air at a known velocity, and a jack for raising and lowering the column so that different heights in the bed could be investigated. These accessories will be discussed in this order.

Distributor Assembly. The air was distributed by the distributor assembly shown in Fig. 3. The air first passed through an 8-inch calming section of $\frac{1}{4}$-inch ceramic spheres. Above the bed of ceramic spheres, the air was distributed by a canvas filter cloth positioned between two 20-mesh wire screens. This provided for a fine dispersion of air. The two wire screens and filter cloth were positioned between the lower flange of the column and a second lucite flange similar to the lower flange of the column. The pressure drop across the distributor was taken from the pressure taps in these two flanges.

Manometers. A 30-inch manometer using water as the manometer fluid was used to measure the pressure drop over the column. A 20-inch, U-shaped manometer using a manometer oil with specific gravity of 0.818 was used for measuring the pressure drop across the distributor.

Air Supply. A compressed-air line from the Kansas State University Physical Plant provided air for fluidizing. The flow rate of air was measured by using a rotameter. A stainless steel float was used for air velocities of 90 ft./min. or greater, while an aluminum float was used for velocities below 90 ft./min. The rotameter was calibrated at various pressure readings by means of Anemostat Corporation of America Anemotherm. The Anemotherm had been previously calibrated with a wet-test meter. The air was dried by passing it through a silica-gel air dryer.

Jack Assembly. The column-distributor assembly was mounted on an iron frame which was raised and lowered by means of a hand jack making it possible to investigate various heights in the column.

<u>Gamma-ray Source and Nuclear Instrumentation</u>. Two gamma-ray sources were used to provide a greater intensity, thereby increasing the count rate and improving the statistics. These two sources were a five millicurie Ra^{226} source and a twenty-five millicurie Cs^{137} source. The two sources were placed in a 5/8-inch hole drilled lengthwise in a 2x4x8-inch lead brick. The 5/8-inch hole served as a collimator for the γ-radiation from the two sources. For added shielding other lead bricks were placed around the brick containing the source. The beam was directed through the center of the column. On the opposite side of the column a 7/16-inch diameter collimator transmitted the beam to the scintillation probe which was positioned directly behind the collimator. This collimator consisted of two bricks with the hole drilled through the 2-inch width of the bricks. This was done so that the 8-inch side of the bricks could be used to shield the probe from stray radiation. A close-up view of the source, collimators, column, and probe is shown in Fig. 7.

Instrumentation for the measurement, detection, and the

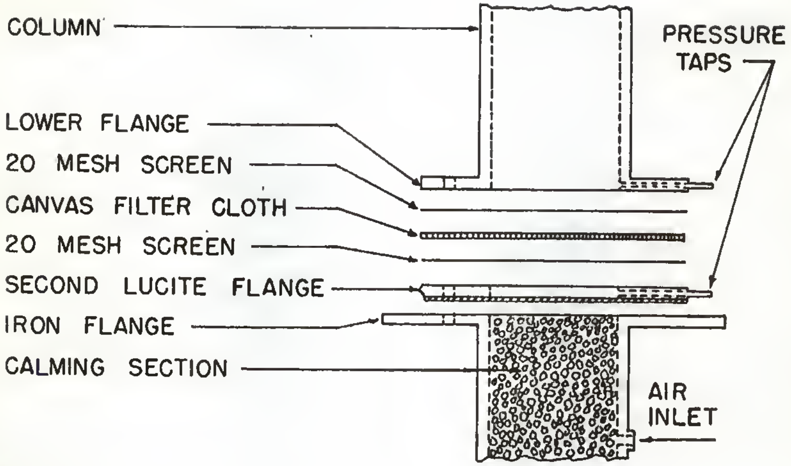

Fig. 3. Distributor assembly.

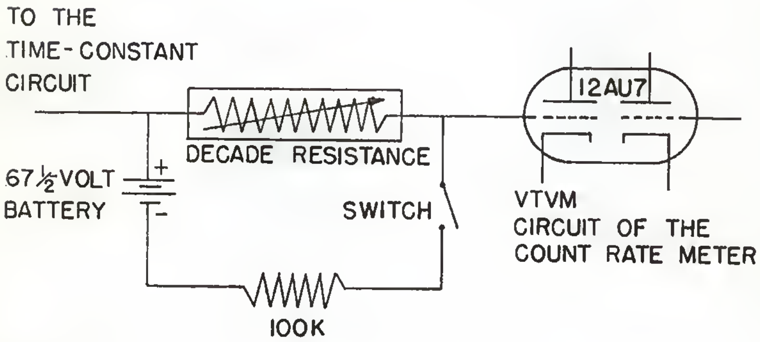

Fig. 4. Bucking-voltage circuit.

recording of the transmitted gamma-radiation included a scintillation probe, power supply, modified count rate meter, bucking voltage supply, and recorder. These instruments will be discussed in this order.

Scintillation Probe. The probe, a Model DP3, B-J Electronics, Borg-Warner Corporation, was used without modification. This instrument consisted of a Type 704, thallium-activated sodium iodide scintillation crystal, a Type 6292, DuMont photomultiplier tube, and a one-tube (6AK5) preamplifier. The probe was operated at 1200 volts.

Power Supply. A John Fluke Mfg. Co. Model 400BDA high-voltage power supply was used for operation of the scintillation probe.

Modified Count Rate Meter. The scintillation probe output was fed into a B-J Electronics Model DM1-D count rate meter that had been slightly modified. The rate meter was equipped with five scale multiplication constants; 10, 30, 100, 300, and 1000. After adding a 0.3-second and a 1-second time constant, the meter included five time constants, 0.3, 1, 3, 10, and 30 seconds. Only the 0.3-second and 30-second time constants were used. Either the 300 or 1000 scale multipliers could have been used; however, the 300 was chosen since it made the measurement more sensitive, i.e., the same deviation on the 300 scale appeared 3.3 times as great as on the 1000 scale. In choosing the 300 scale multiplier it bacame necessary to modify the rate meter. With the high activity used, it was necessary to apply a bucking voltage in order that the CRM would read on-scale, and so that the full range of density fluctuations could be covered. To the input of the vacuum-tube voltmeter circuit of the CRM, the bucking voltage was added. This bucking voltage acted as a negative bias on the input grid of the voltmeter circuit. (Fig. 4).

Recorder. This instrument, an Esterline-Angus Model AW graphic ammeter was used without modification. The recorder was connected in series with the CRM.

Materials

Spherical glass beads obtained from the Minnesota Mining and Manufacturing Co. were used exclusively. The beads were of two sizes, 40-45 mesh and 80-100 mesh. The 40-45 mesh beads ranged in size from 0.0138 inches to 0.0164 inches in diameter while the 80-100 mesh beads ranged in size from 0.0049 inches to 0.0070 inches in diameter. The material of the beads had a density of 2.47 g./cc. The beads were reclassified and oven-dried each time the bed was changed.

Calibrations

Before any useful experimental results could be obtained, it was necessary to calibrate the instruments so that the radiation attenuation technique would be accurate. In using the 300 scale multiplier of the count rate meter, it was necessary to calibrate the density vs. recorder reading for several different bucking voltages. This was done so that the full range of densities, i.e., empty bed to packed bed, could be covered without the CRM going off scale. The calibration curves were made to overlap to some extent.

Calibration Technique. Spacers similar to that shown in Fig. 5 were used in making the average density-recorder reading calibration. These spacers were designed to fit snugly into the column. The column was filled with glass beads of a known packed density. Spacers of various width were then inserted perpendicular to the γ-ray beam. The spacers were made from very thin sheet metal and had inside air-gap widths of 0.25, 0.50, 0.75, 1.00, 1.25, 1.50, and 2.00 inches. The process was also reversed, i. e., beads were put inside the spacers, and the area surrounding the spacers was empty. Each time the γ-ray beam had to pass through the walls of the column. The wall thickness was constant; therefore, the portion of the beam attenuated by the column could be disregarded since it was the same for all cases. When spacers were inserted, the beam was partially attenuated by two thicknesses of the sheet metal. It was therefore necessary to position two thicknesses of sheet metal in front of the collimator opening when spacers were not used. Figures 6 and 7 illustrate these two situations. The density corresponding to a particular spacer was calculated from the following relations.

$$(\text{Density packed}) \times \left(\frac{R_c - R_s}{R_c}\right)$$, when the beads were outside the spacer,

Fig. 5. Calibration spacer.

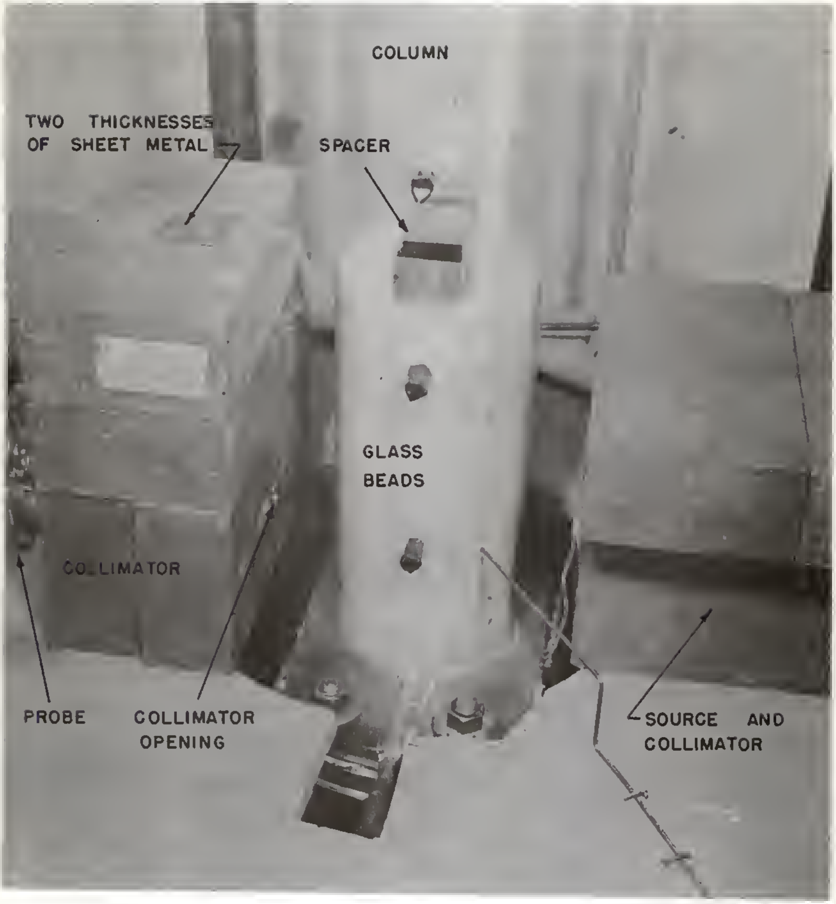

Fig. 6. Calibration technique with spacer inserted.

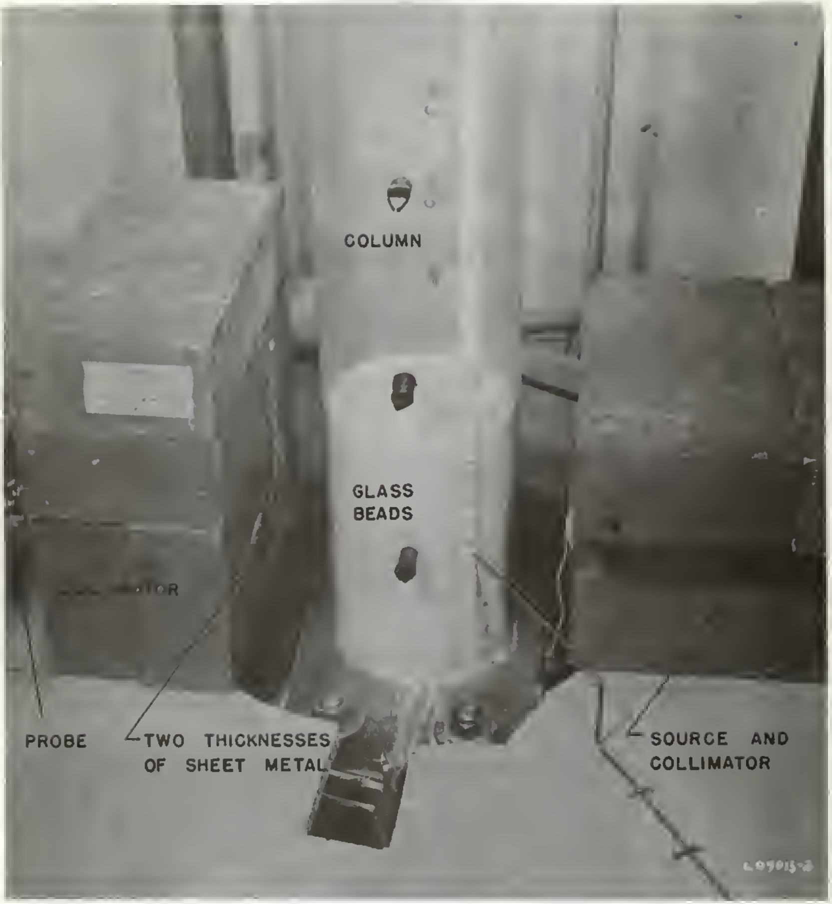

Fig. 7. Bed arrangement with spacer out.

and

$$(\text{Density packed}) \times \left(\frac{R_s}{R_c}\right)$$, when the beads were inside the

spacer.

The packed density of the bed was 1.52 g./cc.; R_c, the column width, was 3.97 inches; and R_s, the width of the spacer, corresponded to the spacer used. In using these relations it was assumed that the density of air was negligible, and that the thickness of the spacer wall was negligible. These assumptions were quite satisfactory for the purposes of this investigation. The calculated densities corresponding to various spacers are presented in Table 1.

Table 1. Densities corresponding to various spacers.

Spacer	Calculated density (g./cc.)
Densely packed bed	1.520
0.25-inch, beads out	1.424
0.50-inch, beads out	1.329
0.75-inch, beads out	1.233
1.00-inch, beads out	1.137
1.25-inch, beads out	1.041
1.50-inch, beads out	0.946
2.00-inch, beads out	0.754
2.00-inch, beads in	0.766
1.50-inch, beads in	0.574
1.25-inch, beads in	0.479
1.00-inch, beads in	0.383
0.75-inch, beads in	0.287
0.50-inch, beads in	0.191
0.25-inch, beads in	0.096
Empty column	0.0

In addition, the calibration was checked before each experimental run was made.

The density-recorder reading calibration was made using both the 0.3-second and the 30-second time constants. The 30-second time constant trace was relatively constant and could be read directly from the strip chart; however, the 0.3-second calibration data showed considerable fluctuation and were averaged over 40 readings to give a large sampling which was required by the statistical approach.

During this investigation the 25 millicurie cesium source was replaced because it was suspected of leaking. Therefore, the equipment was recalibrated. The two sets of calibration curves are presented in Figure 8 and 9.

<u>Average Density - Variance Calibration</u>. A second type of calibration was made. This was done for the statistical approach. After the density-recorder reading calibration was made, the 0.3-second calibration data were used to calculate the variance (standard deviation squared) in apparent density for packed beds of average densities corresponding to the various spacers. These fluctuations in the apparent density were due to the statistical nature of radioactive decay. A linear regression technique was used to fit the best straight line through the calibration points. The relation used was

$$\sigma_p^2 = A + B\bar{\rho}$$

where A was the variance intercept and B was the slope of the

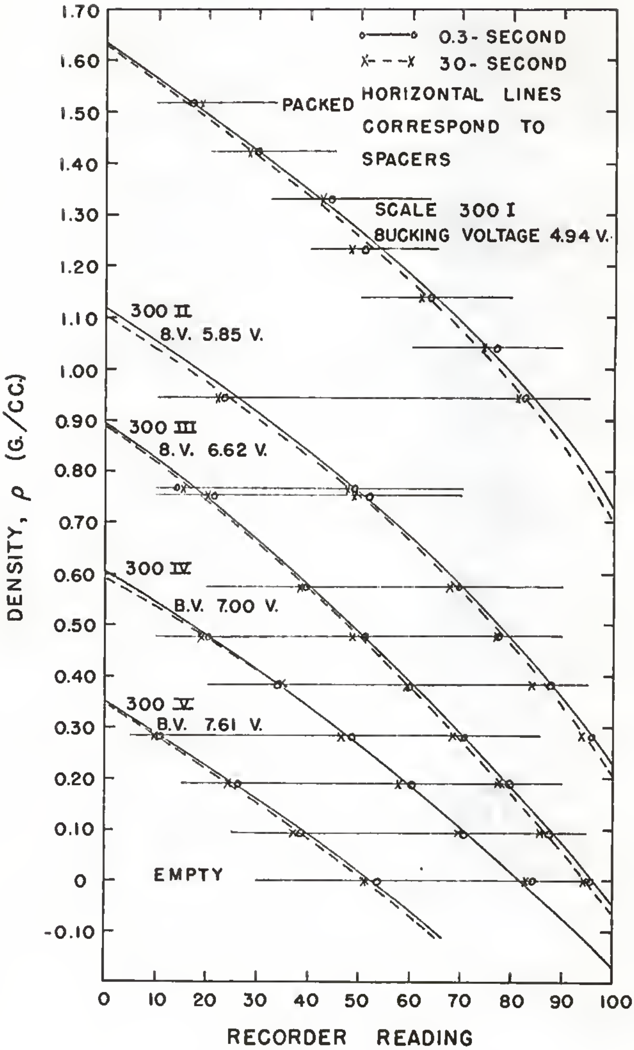

Fig. 8. Density - recorder reading calibration (#1).

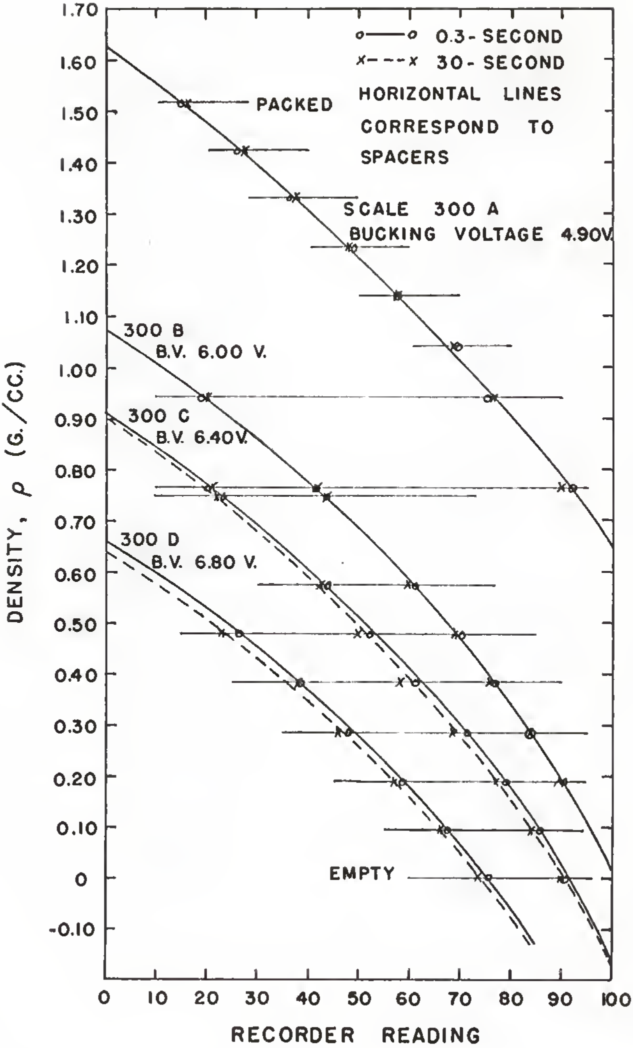

Fig. 9. Density - recorder reading calibration (#2).

line. This type of calibration was also repeated when the 25 millicurie cesium source was replaced. The constants A and B are tabulated below, and the curves are shown in Figures 10 and 11.

Table 2. Constants A and B from linear regression.

	A	B
Calibration #1 Runs 1 - 8	0.0004288	0.0006108
Calibration #2 Runs 9 - 38	0.0003812	0.0004915

Procedure

The instrumentation was set, and the calibration was checked. The column was loaded with the desired particle mixture. The air velocity was set, and a vertical traverse of the fluidized bed was made. Data were generally taken at every half-inch in the bed, starting at one inch above the distributor. Near the top of the fluidized bed, data were taken every quarter-inch in order to better define the expanded bed. The data were taken on both the 0.3-second and the 30-second time constants, and the bucking voltage appropriate for the particular density range. The recorder was allowed to run for about one minute on the 0.3-second time constant so that a large sampling (forty) of densities could be obtained. All electronic equipment remained on 24 hours per day to provide stability in the system.

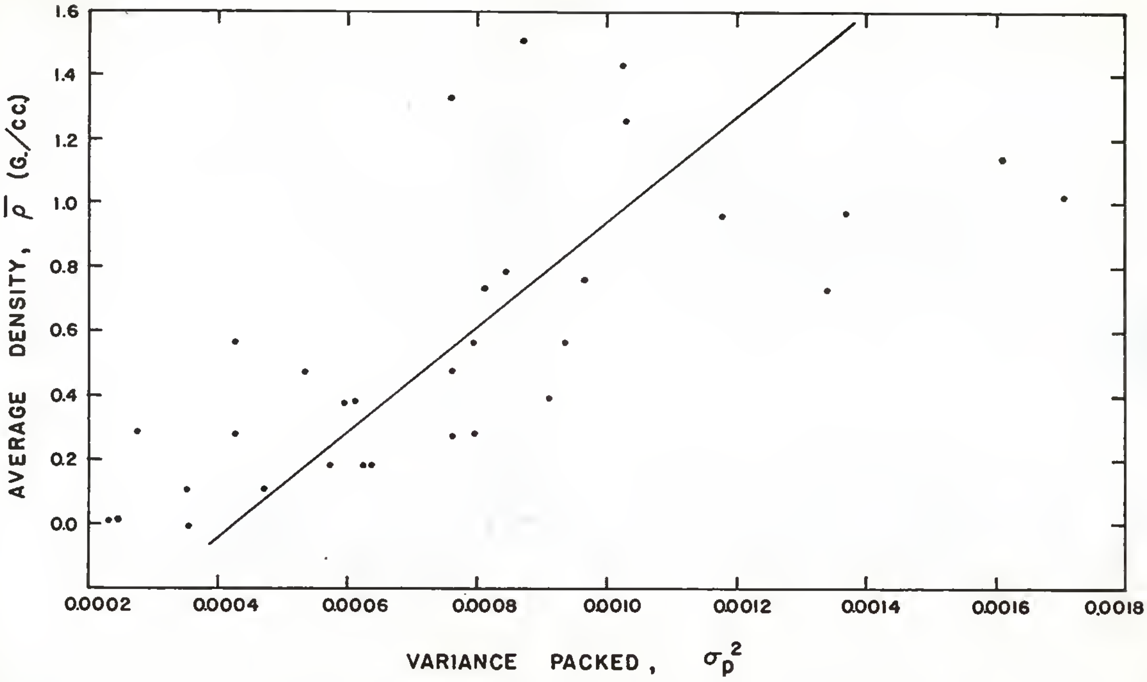

Fig. 10. Average density - variance calibration (#1).

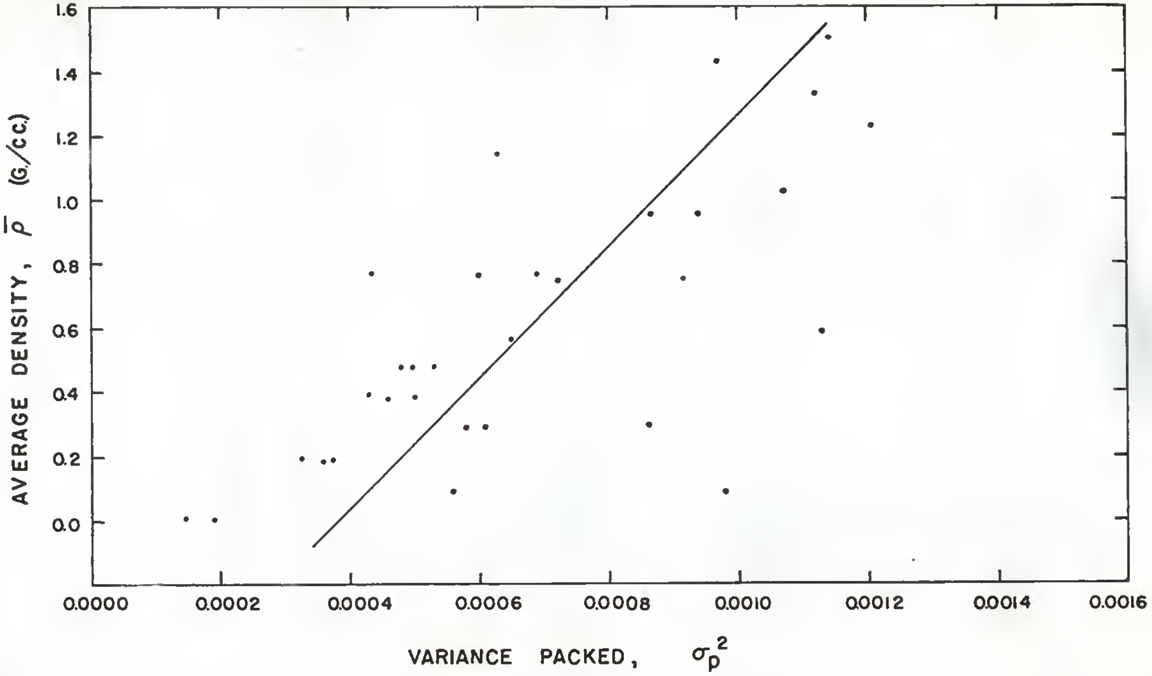

Fig. II. Average density - variance calibration (#2).

BED QUALITY AND THE STATISTICAL APPROACH

Previoue Investigatione

Short time-constant data for determining bed quality have been treated in numerous manner by other research workers. Most of these inveetigators have defined a quality index based upon the percent deviation in some bed property divided by the bubble frequency. Morse and Ballou (8) used the capacitance probe method for determining bed uniformity. They defined an index of uniformity as percent deviation in density divided by the bubble frequency. Dotson (2) also used the capacitance probe method and defined a non-uniformity index as the variation in density divided by the average density expreesing the result ae a percentage. Shuster and Kisliak (12) defined the uniformity index as the average pressure drop divided by the bubble frequency. All of these investigators used an average value from which deviations could be measured. Recently Romero (11), ueing a hot-wire anemometer, defined a quality index as a constant times the sum of peak side lengths divided by the frequency cubed. Thie was actually an average area divided by frequency, and therefore, similar to the definition of Morse and Ballou, and Shuster and Kisliak.

Morse and Ballou, and Dotson by inserting a capacitance probe into the fluidized bed were creating an additional disturbance to which extent was indeterminable.

With the exception of Dotson, who did not use bubble frequency, it was generally necessary for these investigators to decide which deviations were bubbles and which were not, i. e., equipment variations, etc. This made their determinations less quantitative because of the uncertainty involved.

It is suggested here that a more reasonable and necessary approach would be statistical in nature. The statistical approach was chosen because the methods used in statistics are specifically prescribed for observational data. In addition, the statistical treatment of data is widely accepted. In choosing the statistical approach, it was kept foremost in mind that the ultimate goal was in defining an index of stability and uniformity for the fluidized bed. It was also desirous to include a criterion by which data could be judged for their acceptability.

General Consideration

The works of Fisher (3) and Snedecor (13) proved quite valuable in outlining this statistical approach.

One of the most practical uses of statistics is in the study of variation. This is extremely convenient because this is the situation present in observing a fluidized bed, i. e., the change or variation from packed to fluidized. However, before any tests of variance can be used on a sampled population, it must be proved that the sample is distributed in the same distribution upon which the test of variance is based. The simplest and best known distribution is the normal distribution. All of the statistics used in this study of bed uniformity and stability tend to be normally distributed for large samples. From this standpoint, the first step in the data analysis is to show that the sample is normally distributed.

Test of Normality

Two types of departure from normality are frequently considered. These are asymmetry or skewness and kurtosis. In the first case, the data are asymmetrically distributed, i. e., the mean and median are different. The second type of departure from normality, kurtosis, is characterized by either an excess or deficit of items near the center of the range. These departures are illustrated in Figure 12. In making the tests for departure from normality the third and fourth powers of the deviations from the mean are used, the third power for asymmetry, the fourth power for kurtosis.

The relationships used in testing for these departures from normality follow.

<u>Statistics Derived From Sums of Powers</u>. If x_i is the variate of which N observations are made, the sums of powers of the observed values are:

$$s_1 = \sum_{i=1}^{N} (x_i) \qquad s_2 = \sum_{i=1}^{N} (x_i^2)$$

$$s_3 = \sum_{i=1}^{N} (x_i^3) \qquad s_4 = \sum_{i=1}^{N} (x_i^4),$$

and the average or mean is given by

$$\bar{x} = \frac{s_1}{N} . \tag{1}$$

The sums of powers of the deviations from the mean are given by

$$S_2 = s_2 - \frac{1}{N} s_1^2 \tag{2}$$

$$S_3 = s_3 - \frac{3}{N} s_2 s_1 + \frac{2}{N^2} s_1^3$$

$$S_4 = s_4 - \frac{4}{N} s_3 s_1 + \frac{6}{N^2} s_2 s_1^2 - \frac{3}{N^3} s_1^4 .$$

<u>k-statistics</u>. The k-statistics needed are based upon the above relations and are given by

$$k_1 = \frac{1}{N} s_1$$

$$k_2 = \frac{1}{N-1} S_2$$

$$k_3 = \frac{N}{(N-1)(N-2)} S_3$$

$$k_4 = \frac{N}{(N-1)(N-2)(N-3)} \left[(N+1)S_4 - 3\,\frac{N-1}{N}\,S_2^{\,2} \right].$$

__g-statistics and Standard Error of g-statistics Derived From Samples of N Observations.__ The two measures of departure from normality are determined from the g-statistics. The g-statistics are functions of the k-statistics and are given by

$$g_1 = k_3/k_2^{3/2} \quad \text{for asymmetry or skewness, and}$$

$$g_2 = k_4/k_2^{\,2} \quad \text{for kurtosis.}$$

The sampling variance or standard error squared of g is a function of only the number of observational data and is given by

$$\sigma_{g_1}^{*2} = \frac{6N(N-1)}{(N-2)(N+1)(N+3)} \quad \text{for } g_1\text{, and}$$

$$\sigma_{g_2}^{*2} = \frac{24N(N-1)^2}{(N-3)(N-2)(N+3)(N+5)} \quad \text{for } g_2\,.$$

The g-statistic is normally distributed about its mean which is zero. A positive g_1 indicates a skewness such that the mean is greater than the median, while a negative g_1 indicates the opposite. A positive g_2 indicates an excess of items near the mean and far from it, with a corresponding deficit in between. A negative g_2 indicates a flat-topped distribution.

The ultimate criterion for deciding whether or not the departure from normality is significant is based upon the ratio,

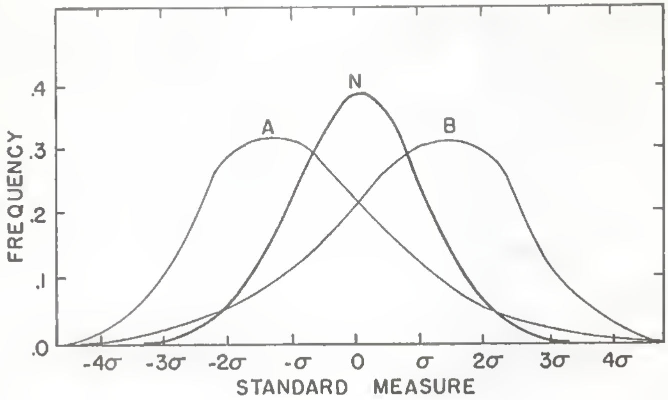

a. Skewness. A, mean greater than median (g_1 positive); B, median greater than mean (g_1 negative); N, normal curve ($g_1 = 0$).

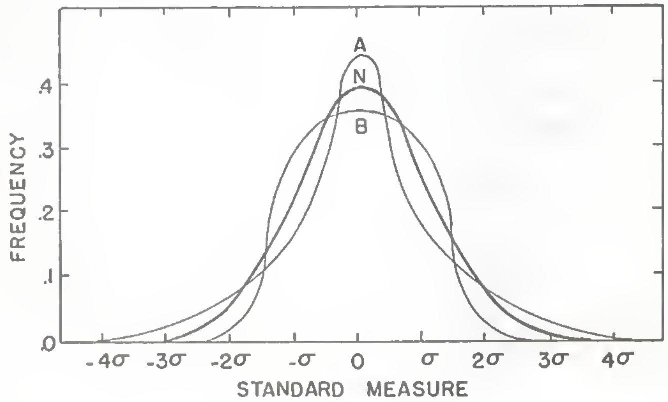

b. Kurtosis. A, g_2 positive; B, flat-topped distribution (g_2 negative); N, normal curve ($g_2 = 0$).

Fig. 12. Departures from normality.

$$y = \frac{\bar{x} - m}{\sigma_x^*} \quad ,$$

where $\bar{x}$ is the average value of the statistic investigated, and m is the median. The relation becomes

$$y = \frac{g - 0}{\sigma_g^*}$$

since the median for the g-statistic is zero. The commonly accepted criterion for significance is the 5 percent level. The value for y at the 5 percent level is 1.960. This means that the departure from normality is not significant unless the value of g is more than 1.960 times the standard error, σ_g^*, of the g-statistic.

These relations were used in showing that the observational data from the fluidized bed were of the normal form. Fifty data points were taken from each of six bed conditions. Two of these were on the packed bed, while the remaining four were from beds fluidized with low and high gas velocities. It was expected that the static bed data would be normally distributed since it is known that radioactive decay follows the normal distribution. However, there was some question as to whether the fluidized bed data would be normally distributed. The results of these tests for normality are given in Tables 3-8. All tests resulted in values of y well below the critical value of 1.960, indicating that the sampled populations were normally distributed and could be analyzed statistically.

Table 3. Normality test for packed bed.

N	x_i	x_i^2	x_i^3	x_i^4	N	x_i	x_i^2	x_i^3	x_i^4
1	8.0	64.00	512.000	4096.0000	33	4.0	16.00	64.000	256.0000
2	8.0	64.00	512.000	4096.0000	34	5.0	25.00	125.000	625.0000
3	9.0	31.00	729.000	6561.0000	35	9.0	81.00	729.000	6561.0000
4	2.5	6.25	15.625	39.0625	36	6.0	36.00	216.000	1296.0000
5	8.6	73.96	636.056	5470.0816	37	7.0	49.00	343.000	2401.0000
6	8.6	73.96	636.056	5470.0816	38	3.0	9.00	27.000	81.0000
7	6.5	42.25	274.625	1785.0625	39	6.0	36.00	216.000	1296.0000
8	6.0	36.00	216.000	1296.0000	40	11.2	125.44	1404.928	15735.1936
9	5.2	27.04	140.608	731.1616	41	4.5	20.25	91.125	410.0625
10	6.0	36.00	216.000	1296.0000	42	1.3	1.69	2.197	2.8561
11	10.0	100.00	1000.000	10000.0000	43	4.8	23.04	110.592	530.8416
12	8.3	68.84	571.787	4745.8321	44	9.0	81.00	729.000	6561.0000
13	4.0	16.00	64.000	256.0000	45	6.0	36.00	216.000	1296.0000
14	8.0	64.00	512.000	4096.0000	46	3.2	19.24	32.768	104.8576
15	6.2	38.44	238.328	1477.6336	47	6.2	38.44	238.328	1477.6336
16	12.1	146.41	1771.561	21435.8881	48	5.2	27.04	140.608	731.1616
17	10.0	100.00	1000.000	10000.0000	49	5.2	27.04	140.608	731.1616
18	4.0	16.00	64.000	256.0000	50	2.1	4.41	9.261	19.4481
19	9.0	81.00	729.000	6561.0000					
20	8.0	64.00	512.000	4096.0000	s	325.9	2436.27	19892.923	173320.7355
21	6.0	36.00	216.000	1296.0000			-2124.22	-47638.820	-518648.2100
22	7.5	56.25	421.875	3164.0625				27691.280	621019.7000
23	7.8	60.84	474.522	3701.5056					-270737.6700
24	6.0	36.00	216.000	1296.0000					
25	5.0	25.00	125.000	625.0000	S		312.05	-54.62	4954.56
26	4.2	17.64	74.088	311.1696					
27	10.1	102.01	1030.301	10406.0601	k	6.52	6.37	1.16	-15.00
28	8.0	64.00	512.000	4096.0000					
29	7.3	53.29	389.017	2839.8241	g	0.07	-0.37		
30	1.2	1.44	1.728	2.9736					
31	6.0	36.00	216.000	1296.0000	σ_g^*	0.3366	0.6619		
32	10.1	102.01	1030.301	10406.0401	y	0.21	-0.56		

Table 4. Normality test for packed bed.

N	x_1	x_1^2	x_1^3	x_1^4	N	x_1	x_1^2	x_1^3	x_1^4
1	6.0	36.00	216.000	1296.0000	33	8.1	65.61	531.441	4304.6721
2	6.0	36.00	216.000	1296.0000	34	6.0	36.00	216.000	1296.0000
3	7.5	56.25	421.875	3164.0625	35	4.2	17.64	74.088	311.1696
4	6.0	36.00	216.000	1296.0000	36	5.0	25.00	125.000	625.0000
5	9.9	98.01	970.299	9605.9601	37	10.2	104.04	1061.208	10824.3216
6	3.0	9.00	27.000	81.0000	38	7.1	50.41	357.911	2541.1681
7	12.5	156.25	1953.125	24414.0625	39	7.3	53.29	389.017	2839.8241
8	8.0	64.00	512.000	4096.0000	40	10.0	100.00	1000.000	10000.0000
9	9.0	81.00	729.000	6561.0000	41	10.0	100.00	1000.000	10000.0000
10	9.3	86.49	804.357	7480.5201	42	6.0	36.00	216.000	1296.0000
11	9.0	81.00	729.000	6561.0000	43	7.0	49.00	343.000	2401.0000
12	12.0	144.00	1728.000	20736.0000	44	11.3	127.69	1442.897	16304.7361
13	5.3	28.09	148.877	789.0481	45	7.7	59.29	456.553	3515.3041
14	4.0	16.00	64.000	256.0000	46	5.0	25.00	125.000	625.0000
15	9.0	81.00	729.000	6561.0000	47	6.2	38.44	238.328	1477.6336
16	7.1	50.41	357.911	2541.1681	48	4.2	17.64	74.088	311.1696
17	8.0	64.00	512.000	4096.0000	49	10.0	100.00	1000.000	10000.0000
18	6.0	36.00	216.000	1296.0000	50	8.0	64.00	512.000	4096.0000
19	6.0	36.00	216.000	1296.0000					
20	4.0	16.00	64.000	256.0000	s	375.3	3119.03	27923.853	264533.5007
21	6.0	36.00	216.000	1296.0000			-2817.00	-70234.32	-838385.67
22	9.2	34.64	778.688	7163.9296				42288.83	1054357.57
23	2.3	5.29	12.167	27.9841					-476129.95
24	10.0	100.00	1000.000	10000.0000					
25	8.0	64.00	512.000	4096.0000	S		302.03	-21.64	4375.45
26	12.3	151.29	1860.867	22888.6641					
27	7.5	56.25	421.875	3164.0625	k	7.51	6.16	-0.46	-20.38
28	9.0	81.00	729.000	6561.0000					
29	7.0	49.00	343.000	2401.0000	g	-0.03	-0.54		
30	3.0	9.00	27.000	81.0000					
31	10.1	102.01	1030.01	10406.0401	σ_g^*	0.3366	0.6619		
32	10.0	100.00	1000.000	10000.0000					
					y	-0.09	-0.82		

Table 5. Normality test for fluidized bed with low gas flow rate.

N	x_i	x_i^2	x_i^3	x_i^4	N	x_i	x_i^2	x_i^3	x_i^4
1	12.0	144.00	1728.000	20736.0000	33	10.0	100.00	1000.000	10000.0000
2	12.3	151.29	1860.867	22888.6641	34	4.2	17.64	74.088	311.1696
3	13.6	184.96	2515.456	34210.2016	35	6.0	36.00	216.000	1296.0000
4	4.0	16.00	64.000	256.0000	36	6.3	39.69	250.047	1575.2961
5	2.0	4.00	8.000	16.0000	37	7.0	49.00	343.000	2401.0000
6	5.3	28.09	148.877	789.9481	38	3.2	10.24	32.768	104.8576
7	9.0	81.00	729.000	6561.0000	39	9.2	84.64	778.688	7163.9296
8	4.2	17.64	74.088	311.1696	40	7.3	53.29	389.017	2839.8241
9	6.0	36.00	216.000	1296.0000	41	5.0	25.00	125.000	625.0000
10	9.0	81.00	729.000	6561.0000	42	12.0	144.00	1728.000	29736.0000
11	7.0	49.00	343.000	2401.0000	43	10.0	100.00	1000.000	10000.0000
12	10.0	100.00	1000.000	10000.0000	44	5.5	30.25	166.375	915.0625
13	5.2	27.04	140.608	731.1616	45	6.0	26.00	216.000	1296.0000
14	8.0	64.00	512.000	4096.0000	46	8.0	64.00	512.000	4096.0000
15	11.8	139.24	1643.032	19387.7776	47	2.3	5.29	12.167	27.9841
16	2.3	5.29	12.167	27.9841	48	9.0	81.00	729.000	6561.0000
17	8.2	67.24	551.368	4521.2176	49	8.5	72.25	614.125	5220.0625
18	11.1	123.21	1367.631	15180.7041	50	8.5	72.25	614.125	5220.0625
19	8.0	64.00	512.000	4096.0000					
20	4.0	16.00	64.000	256.0000	s	372.1	3254.03	31341.403	323562.0191
21	6.0	36.00	216.000	1296.0000			-2769.17	-72649.47	-932970.80
22	0.0	00.00	000.000	0000.0000				41216.30	1081314.77
23	10.0	100.00	1000.000	10000.0000					-460097.55
24	13.5	182.25	2460.375	33215.0625					
25	8.7	75.69	658.503	5728.9761	S		484.86	-91.77	11808.44
26	5.3	28.09	148.877	789.0481					
27	4.2	17.64	74.088	311.1696	k	7.44	9.90	-1.95	-40.22
28	6.3	39.69	250.047	1575.2961					
29	8.0	64.00	512.000	4096.0000	g	-0.06	-0.41		
30	8.3	68.89	571.787	4745.8321					
31	9.3	86.49	804.347	7489.5201	σ_g^*	0.3366	0.6619		
32	12.0	144.00	1728.000	20736.0000	y	-0.18	-0.62		

Table 6. Normality test for fluidized bed with low gas flow rate.

N	x_1	x_1^2	x_1^3	x_1^4	N	x_1	x_1^2	x_1^3	x_1^4
1	4.5	20.25	91.925	410.0625	33	8.7	75.69	658.503	5728.9761
2	8.0	64.00	512.000	4096.0000	34	2.0	4.00	8.000	16.0000
3	7.2	51.84	373.248	2687.3856	35	3.8	14.44	54.872	208.5136
4	6.0	36.00	216.000	1296.0000	36	11.0	121.00	1331.000	14641.0000
5	5.5	30.25	166.375	915.0625	37	7.0	49.00	343.000	2401.0000
6	8.0	64.00	512.000	4096.0000	38	13.0	169.00	2197.000	28561.0000
7	8.0	64.00	512.000	4096.0000	39	2.0	4.00	8.000	16.0000
8	9.8	96.04	941.192	9223.6816	40	7.5	56.25	421.875	3164.0625
9	3.0	9.00	27.000	81.0000	41	6.2	38.44	238.328	1477.6336
10	7.5	56.25	421.875	3164.0625	42	6.8	46.24	314.432	2138.1376
11	6.0	36.00	216.000	1296.0000	43	10.0	100.00	1000.000	10000.0000
12	14.2	201.64	2863.288	40658.6896	44	12.0	144.00	1728.000	20736.0000
13	10.0	100.00	1000.000	10000.0000	45	11.5	132.25	1520.875	17490.0625
14	9.0	81.00	729.000	6561.0000	46	14.0	196.00	2744.000	38416.0000
15	8.7	75.69	658.503	5728.9761	47	10.0	100.00	1000.000	10000.0000
16	1.0	1.00	1.000	1.0000	48	16.0	256.00	4096.000	65536.0000
17	4.0	16.00	64.000	256.0000	49	10.0	100.00	1000.000	10000.0000
18	11.0	121.00	1331.000	14641.0000	50	12.5	156.25	1953.125	24414.0625
19	4.0	16.00	64.000	265.0000					
20	8.0	64.00	512.000	4096.0000	s	410.6	3966.62	42568.604	493720.2938
21	8.7	75.69	658.503	5728.9761			-3371.85	-97721.65	-1398293.37
22	8.0	64.00	512.000	4096.0000				55379.22	1604980.38
23	4.8	23.04	110.592	530.8416					- 682161.21
24	5.0	25.00	125.000	625.0000					
25	5.2	27.04	140.608	731.1616	S		594.77	226.17	18246.09
26	8.5	72.25	614.125	5220.0625					
27	11.0	121.00	1331.000	14641.0000	k	8.21	12.14	4.81	-49.52
28	6.0	36.00	216.000	1296.0000					
29	15.0	225.00	3375.000	50625.0000	g	0.11	-0.34		
30	8.8	77.44	681.472	5996.9536					
31	9.2	84.64	778.688	7163.9296	σ_g^*	0.3366	0.6619		
32	13.0	169.00	2197.000	28561.0000					
					y	0.33	-0.51		

Table 7. Normality test for fluidized bed with high gas flow rate.

N	x_1	x_1^2	x_1^3	x_1^4	N	x_1	x_1^2	x_1^3	x_1^4
1	23.0	529.00	12167.000	279841.0000	33	11.0	121.00	1331.000	14641.0000
2	14.0	196.00	2744.000	38416.0000	34	13.0	169.00	2197.000	28561.0000
3	16.0	256.00	4096.000	65536.0000	35	20.0	400.00	8000.000	160000.0000
4	17.6	309.76	5451.776	95951.2576	36	15.0	225.00	3375.000	50625.0000
5	10.0	100.00	1000.000	10000.0000	37	22.5	506.25	11390.625	256289.0625
6	12.0	144.00	1728.000	29736.0000	38	16.0	256.00	4096.000	65536.0000
7	24.0	576.00	13824.000	331776.0000	39	13.2	174.24	2299.968	30359.5776
8	9.7	94.09	912.673	8852.9281	40	21.7	470.89	10218.313	221737.3921
9	13.5	182.25	2460.375	33215.0625	41	24.0	576.00	13824.000	331776.0000
10	10.2	104.04	1061.208	10824.3216	42	16.0	256.00	4096.000	65536.0000
11	20.0	400.00	8000.000	160000.0000	43	22.0	484.00	10648.000	234256.0000
12	10.0	100.00	1000.000	10000.0000	44	15.8	249.64	3944.312	62320.1296
13	9.0	81.00	729.000	6561.0000	45	10.5	110.25	1157.625	12155.0625
14	11.0	121.00	1331.000	14641.0000	46	16.0	256.00	4096.000	65536.0000
15	18.0	324.00	5832.000	104976.0000	47	10.0	100.00	1000.000	10000.0000
16	18.2	331.24	6028.568	109719.9376	48	18.3	334.89	6128.487	112151.3121
17	22.0	484.00	10648.000	234256.0000	49	16.0	256.00	4096.000	65536.0000
18	14.0	196.00	2744.000	38416.0000	50	17.0	289.00	4913.000	83521.0000
19	16.5	272.25	4492.125	74120.0625					
20	14.0	196.00	2744.000	38416.0000	s	787.2	13654.32	255028.000	5044970.5980
21	22.3	497.29	11089.567	247297.3441			-12393.68	-644920.84	-16060661.59
22	14.0	196.00	2744.000	38416.0000				390252.10	20307267.48
23	27.0	729.00	19683.000	531441.0000					-9216193.48
24	21.5	462.25	9938.375	213675.0625					
25	14.0	196.00	2744.000	38416.0000	S		1260.64	359.55	75383.01
26	4.5	20.25	91.125	410.0625					
27	6.0	36.00	216.000	1296.0000	k	15.74	25.73	7.64	-374.40
28	20.0	400.00	8000.000	160000.0000					
29	10.0	100.00	1000.000	10000.0000	g	0.06	-0.57		
30	10.7	114.49	1225.043	13107.9601					
31	16.5	272.25	4492.125	74120.0625	σ_g^*	0.3366	0.6619		
32	20.0	400.00	8000.000	160000.0000					
					y	0.18	-0.86		

Table 8. Normality test for fluidized bed with high gas flow rate.

N	x_1	x_1^2	x_1^3	x_1^4	N	x_1	x_1^2	x_1^3	x_1^4
1	8.0	64.00	512.000	4096.0000	33	13.0	169.00	2197.000	28561.0000
2	14.0	196.00	2744.000	38416.0000	34	15.0	225.00	3375.000	50625.0000
3	20.0	400.00	8000.000	160000.0000	35	24.2	585.64	14172.488	342974.2096
4	16.5	272.25	4492.125	74120.0625	36	14.3	294.49	2924.207	41816.1601
5	20.0	400.00	8000.000	160000.0000	37	14.0	196.00	2744.000	38416.0000
6	14.0	196.00	2744.000	38416.0000	38	19.0	361.00	6859.000	130321.0000
7	11.0	121.00	1331.000	14641.0000	39	16.0	256.00	4096.000	65536.0000
8	17.0	209.00	4913.000	83521.0000	40	14.0	196.00	2744.000	38416.0000
9	19.0	361.00	6859.000	130321.0000	41	28.0	784.00	21952.000	614656.0000
10	10.0	100.00	1000.000	10000.0000	42	16.0	256.00	4096.000	65536.0000
11	21.0	441.00	9261.000	194481.0000	43	17.0	289.00	4913.000	83521.0000
12	14.0	196.00	2744.000	38416.0000	44	14.0	196.00	2744.000	38416.0000
13	13.0	169.00	2197.000	28561.0000	45	20.0	400.00	8000.000	160000.0000
14	16.0	256.00	4096.000	65536.0000	46	18.8	353.44	6644.672	124919.8336
15	21.0	441.00	9261.000	194481.0000	47	6.0	36.00	216.000	1296.0000
16	16.0	256.00	4096.000	65536.0000	48	25.0	625.00	15625.000	390625.0000
17	9.0	81.00	729.000	6561.0000	49	14.0	196.00	2744.000	38416.0000
18	14.0	196.00	2744.000	38416.0000	50	26.0	676.00	17576.000	456976.0000
19	12.6	158.76	2000.376	25204.7376					
20	15.0	225.00	3375.000	50625.0000	s	783.2	13332.72	244390.130	4789425.1380
21	15.0	225.00	3375.000	50625.0000			-12268.04	-626531.18	-15312507.99
22	14.0	196.00	2744.000	38416.0000				384333.31	19627968.75
23	12.0	144.00	1728.000	20736.0000					- 9030295.39
24	14.0	196.00	2744.000	38416.0000					
25	12.0	144.00	1728.000	20736.0000	S		1064.68	2192.26	74590.51
26	14.5	210.25	3048.625	44205.0625					
27	18.0	324.00	5832.000	104976.0000	k	15.66	21.73	46.60	213.26
28	18.0	324.00	5832.000	104976.0000					
29	21.0	441.00	9261.000	194481.0000	g	0.46	0.45		
30	8.0	64.00	512.000	4096.0000					
31	13.3	176.89	2352.637	31290.0721	σ_g^*	0.3366	0.6619		
32	8.0	64.00	512.000	4096.0000					
					y	1.37	0.68		

Statistics for Data Analysis

The proof of normality for the sampled population makes it possible to continue the statistical approach. Two well-known statistics which are quite useful are the mean and the variance from the mean. The mean has been previously defined as

$$\bar{x} = \frac{s_1}{N} ,$$

and the variance is the standard deviation squared which is given by

$$\sigma^2 = \frac{S_2}{N-1} \quad . \tag{3}$$

It should be noted that the standard deviation as defined in this case is the estimated standard deviation and is a function of both the variate x_i and the number of observations, N, while σ^*, which has been previously defined, is the standard deviation of the sampling and is a function of only N.

These two well-known statistics are used in the χ^2 test which is used to test the goodness of fit between observation and hypothesis. This test is quite useful in testing whether a sample from a normal distribution confirms or contradicts the variance which it is expected to have. For the variate x_i with known standard deviation, σ_{known},

$$\chi^2_{N-1} = \frac{\sum_{i=1}^{N}(x_i - \bar{x})^2}{\sigma^2_{known}} = \frac{S_2}{\sigma^2_{known}} = \frac{(N-1)\ \sigma^2_{observed}}{\sigma^2_{known}} \tag{4}$$

where N-1 is the degreee of freedom, ν, that characterizee the eample. It ie obvious from the above relation that the nearer are the values of x_i to the mean, the emaller will be χ^2. In other worde smaller deviatione yield smaller χ^2 valuee.

In 1900, K. Pearson established the distribution of χ^2 for any value of ν. This makes it possible to calculate the probability, P, that a particular value for χ^2 will be exceeded. There existe a probability, P, for every value of χ^2. As χ^2 is increaeed from zero to infinity, P decreases from one to zero. The relation between χ^2 and P is a complex one, and tables have been made for this χ^2 dietribution with various degrees of freedom.

The χ^2 statistic, as stated before, is a test to determine how well certain data fit a known or given hypothesis. In practice an exact value for P is not desired, but it ie desirous to know whether or not the data are open to euspicion. The commonly accepted value for P is 0.05, the five percent level. Thie may be interpreted in the following way. Unless the obeerved value of χ^2 is greater than the χ^2 value given by the χ^2 dietribution for a given ν and $P = 0.05$, there is no reason to euspect the hypothesis being tested. On the other hand, in the event that the observed χ^2 is greater, indicating that the probability of this occuring is less than 0.05, one must suspect the tested hypothesis. In the first of these two cases, the value of χ^2 may be interpreted as a sampling variation, while in the second case rejection of the hypothesis is suggested.

This concept is of importance to the fluidized bed because this statistic can provide a criterion for deciding whether or not there is a significant difference between the packed bed state and the fluidized state. For instance, let the packed bed be hypothesized and the fluidized bed be observed. The value for χ^2 should exceed the value given by the tables since it is known that the hypothesis is incorrect. In the event that the observed χ^2 should be less than the statistical value, the data could be rejected owing to the fact that it followed an incorrect hypothesis. Thus the χ^2 test is useful for judging the acceptability of data.

Another statistic which is quite useful in the analysis of two groups of data is the variance ratio, often called the F ratio for its discoverer, Fisher. Fisher tabulated the F distribution for ν and P as was done for the χ^2 distribution. This variance ratio is useful in testing whether or not two groups of data are from the same normal distribution. The test is made by simply taking the ratio of the variance, for the two groups, putting the larger over the smaller. Unless the value for F is greater than the value indicated for a particular ν and P, the samples are considered to be from the same normal distribution. The F ratio is based upon random sampling from normal populations. The F ratio could be used in an analogous manner to the

χ^2 test, providing each sample was taken at random.

Data Analysis

A typical strip-chart recording is presented in Fig. 13. The 30-second time-constant portion was used only to determine the average density for comparison with the 0.3-second time-constant data. For most of the 30-second time-constant data the recorder reading was constant or varied only to a small extent. The average density corresponding to the recorder trace was obtained from the calibration curves for the long time-constant data. For instance, the strip-chart reading of Fig. 13 is 62 on the 300 C scale. From the calibration curve, Fig. 9, this corresponds to an average density of 0.368 g./cc.

The 0.3-second time-constant data were analyzed with the statistical approach. The trace made on the strip chart was the trace of the normally distributed fluidized bed population. It should be noted that this trace would be different for instrumentation (including recorder) with a different response time. Each time this trace crossed one of the curved vertical lines, the population was sampled. Because of the fact that the statistical tests previously described were designed for large samples, the trace was allowed to cross at least forty of the vertical lines. From these recorder readings, the corresponding density was read from the calibration curves for the 0.3-second time-constant data. For instance, the first two points in Fig. 13, indicated with arrows are 37 and 47 on the 300 C scale.

These two points correspond to densities of 0.634 and 0.540, respectively. The forty densities from the recorder trace were then punched on IBM data cards and loaded into the IBM-650 computer for calculation. The 650 program with detailed explanation is presented on page 85. For a particular set of forty densities from the fluidized bed, the computer calculations yielded the following important quantities: the average density, $\bar{\rho}$; the sum of the deviations square, S_2; the variance, σ_p^2, for a packed bed with the same average density as the input data; the ratio of S_2 to σ_p^2 which is χ^2; the variance, σ_f^2, of the fluidized bed, i. e., the variance of the forty input densities; and, the ratio σ_f^2 to σ_p^2 which was defined as the index of stability and uniformity.

The χ^2 test was used to determine the acceptability of data. The value for χ^2_{39} at the 5 percent level is 54.56 (7). With the exception of two extreme conditions, data that yielded an observed χ^2_{39} less than this value were rejected for the variance analysis. This was done because a value less than 54.56 meant that the data followed the hypothesis that the bed was packed which was impossible since all data were taken on the fluidized bed. The two exceptions to this rule were for data taken very near the distributor or in the dispersed phase at the top of the fluidized bed. Data from very near the distributor were not rejected because it was expected that this location would yield small deviations owing to the fact that bubbles had little chance to form (1), and the uniformity of fluidization might be great enough to make the bed appear packed. Data from the dispersed phase near the top were also expected to have small deviations and therefore approximate a packed condition. Actually, this state is near an empty column which is a packed condition with average density near zero.

The remainder of the data analysis consisted of correlations using the computer output. In all of the graphical analysis the data were subjected to a confidence test. The level used for the confidence test was the 5 percent level. This test consisted of examining the data by a linear regression technique and rejecting data that were outside the 5 percent confidence level. This was necessary because of the statistical nature of the study.

Index of Stability and Uniformity

The index of stability and uniformity has been defined as

$$ISU = \frac{\sigma_f^2}{\sigma_p^2} \tag{5}$$

This is obviously a variance ratio, and at first glance appears to be the F ratio previously mentioned. However, it differs slightly in that the denominator, σ_p^2, is not obtained from a random sample, but from the equation,

$$\sigma_p^2 = A + B\bar{\rho} \tag{6}$$

of the variance-average density calibration. The variance of the fluidized bed is from a random sampling; therefore, in the strictest sense, ISU is not the F ratio. Because of this, the F test of significance cannot be used. This in no way affects this study since the χ^2 test is used for a significance test. The ISU eerves the purpose of comparing the unstable fluidized bed to the stable packed bed.

Consider Fig. 17b, where the bed is packed, and the Fig. 13, where the bed is fluidized. In the first case the variance is a result of only the random nature of radioactive decay and is dependent only upon the average density of the bed. In the latter case the variance is due to both the radioactive decay and the disturbance caused by fluidization. The ratio of these variances for a particular average density is then the factor by which the variance is increased due to the fluidizing process, and has been named the index of stability and uniformity.

This index must be defined more precisely so that its meaning will not be misinterpreted. The terms stability and uniformity have been used in the literature in several ways and need explicit definitions before they can be used.

Consider the ideal fluidized bed to be a column with liquid of a constant density in it. This bed has no voids, nor is there any disturbance as in gas-solids fluidization. If a vertical density traverse of this column were made with the radioactive beam, the result would appear as in Fig. 14. The density would be constant while the beam was in the bed and the drop to the density of air, i. e., approximately zero at the bed surface.

The bed could be considered to be of uniform density.

Now consider a vertical ISU traverse. The packed and fluidized states are exactly the same, i. e., there are no disturbances, and the bed could be considered perfectly stable. The variance ratio would vary only slightly from one due to the statistical nature of the variance. For theoretical purposes, the ISU could be considered unity. The vertical profile would then appear as in Fig. 15. The bed could be considered perfectly stable and uniform.

Consider now two non-ideal cases; first, a case where the disturbances are small at the bottom of the column, but increase until they become large at the top; and second, a case where the disturbances are large at the bottom and increase only slightly in going to the top. Examples of these hypothetical cases are shown in Fig. 16. These two cases may be compared in the following manner using the terms stability and uniformity. It may be said that bed "A" is more stable than bed "B"; however, bed "B" is more uniform than bed "A". When this statement is made, it becomes evident that the magnitude of disturbances is smaller in bed "A", and is more constant in bed "B". A small index means less disturbance, more stability and therefore, more uniformity of fluidization. A relatively constant index means less change in the disturbances throughout the column; thus, the disturbance is uniform.

It is important to distinguish between uniformity and uniformity of fluidization. Uniformity refers to the relative constancy of the index, while uniformity of fluidization refers

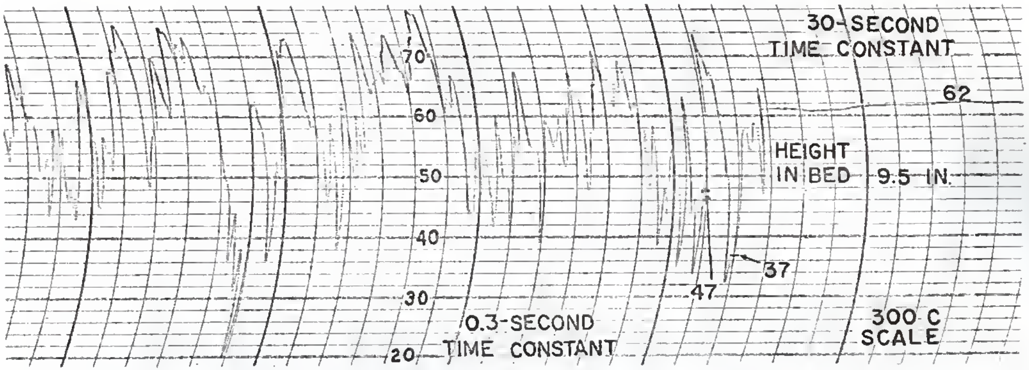

Fig. 13. Typical recorder trace.

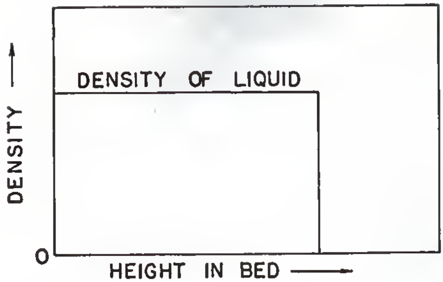

Fig. 14. Vertical density prafile af ideal bed.

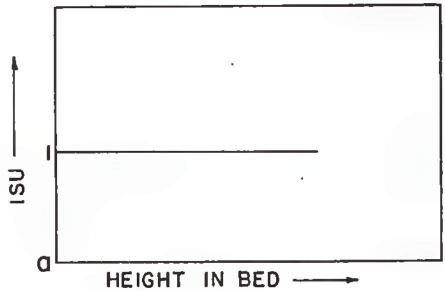

Fig. 15. Vertical ISU prafile of ideal bed.

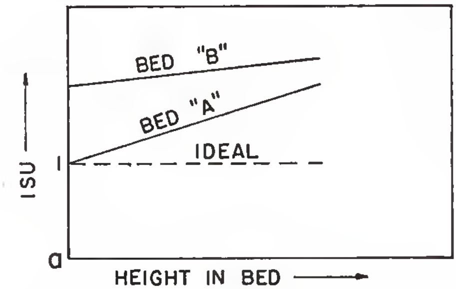

Fig. 16. Vertical ISU profiles for two non-ideal beds.

to magnitude of disturbances, i. e., the stability of the bed. Since the disturbances in a gas-solids system are in the form of bubbles, good stability indicates uniformity of fluidization through small bubbles.

DISCUSSION AND RESULTS

For purposes of clarity this section has been divided into two parts. The first portion concerns general observations, which include calibrations, data acceptability, and comparison of long and short time-constant data. In the second portion, the effects of operational variables upon properties of the fluidized bed are discussed. Observations related to these effects are also presented.

In this investigation, many data points were taken so that a good evaluation of various effects could be made. In previous investigations, definite effects upon bed quality have been hard to evaluate because of an insufficiency of observational data. Over 40,000 data points were read for this investigation, and these are recorded on rolls of strip-chart paper. Since it would be practically impossible to present all of the data, only the reduced data, i. e., computer output, has been presented. These data are tabulated in the appendix with representative samplings discussed in this section.

General Observations

Calibrations. In view of the calibration curves (Figures 8 and 9), the spacer technique for density calibration appears to be quite successful, allowing smooth curves to be drawn through the experimental points. It can be seen that the short and long time-constant calibrations were very nearly the same. This consistency may be regarded as a positive check on the statistical concept of averaging the data points.

Figures 17a and 17b, are sample recorder traces for empty and packed beds. It can be seen that the variance was greater for the packed bed. This results from the fact that smaller count rates, due to a greater attenuation in dense beds, have larger deviations. This can readily be seen by noting that the variance is a function of $\frac{1}{N-1}$, where N, in this case, is the number of counts or count rate. This observation is confirmed in the average density-variance calibrations of Figures 10 and 11.

Acceptability of Data. None of the data were rejected on the basis of the χ^2 test. Values of χ^2_{39} less than 54.56 were obtained in very few cases, and in each case the data were taken near the distributor or at the top of the bed where the χ^2 test did not apply as has been previously explained. The regions "near" the distributor and the "top" of the bed for the test were defined in the following manner. In cases where the value was less than the required value at the lowest level

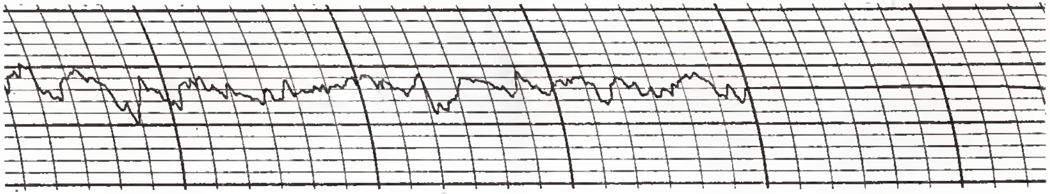

Fig. 17a. Recorder trace for empty bed.

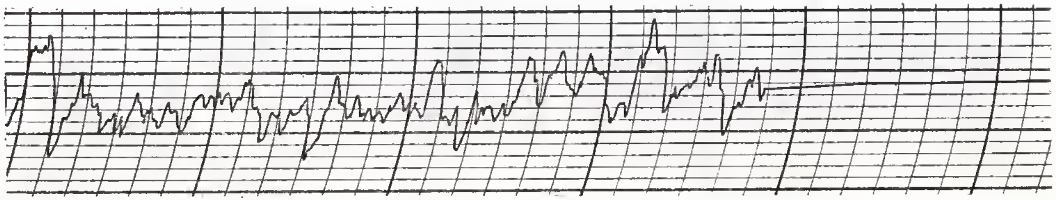

Fig. 17b. Recorder trace for packed bed.

(1 inch), the next height in the bed was checked. This was repeated until the value of χ^2_{39} became greater than 54.56. It was then decided that the region "near" the distributor no longer existed and the χ^2 test was applied. The same process was used for the "top" of the bed. It must be emphasized that this was necessary in very few cases, and these cases occurred when the stability was good, indicating that the bed was actually better represented as in a packed state.

Approximately 10 percent of the data points were rejected by the 5 percent confidence test. The percentage increased with increasing air velocity. This will be explained in detail when the channeling effect is discussed.

<u>Comparison of 0.3-second and 30-second Time Constants</u>. Fig. 18 illustrates vertical mean density profiles taken on the 0.3 and 30-second time constants. It can be seen that the results were almost identical, indicating that the calibration was satisfactory, and that either short or long time-constant data could be used to obtain density profiles in a fluidized bed.

The accuracy of 30-second-time-constant data were checked by Lee (5) who used the same apparatus as this author. This was done by measuring the area under the density profile curve, converting it to weight, and comparing it with the known weight of the bed. This material balance method showed that the error was generally less than 5 percent and in many instances near 1 percent indicating that the radiation attenuation method and calibrations were satisfactory.

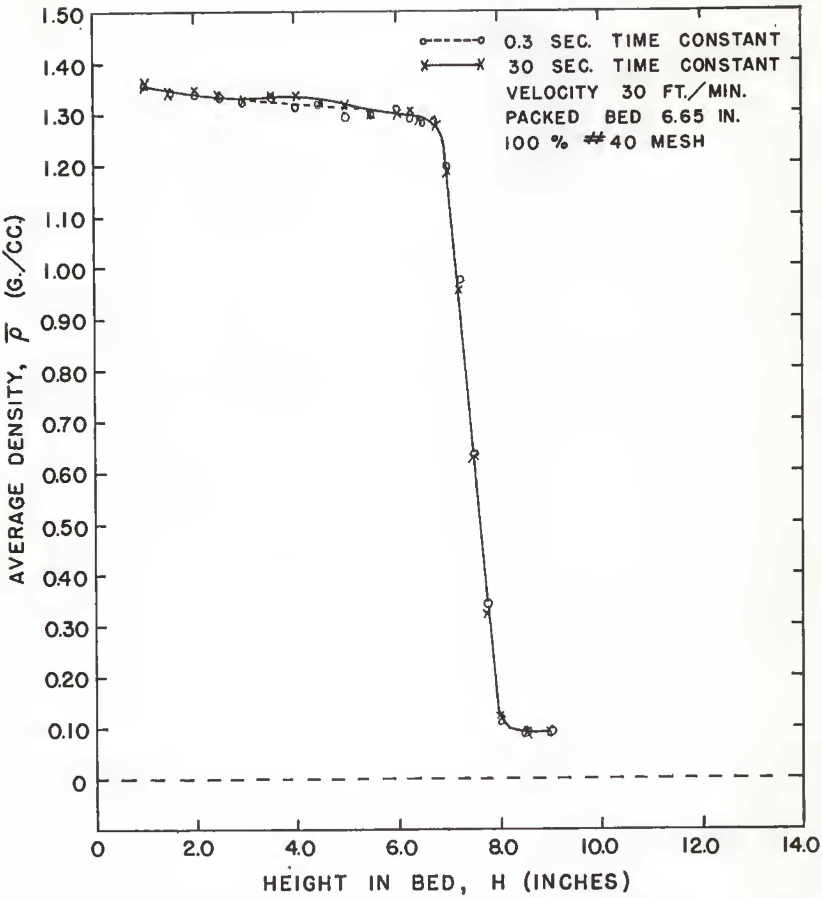

Fig. 18. Comparison of long and short time constants.

Effect of Operational Variables Upon Bed Properties

Effect of Air Velocity and Height in Bed. The effects of air velocity and height in bed upon the average density are shown in Fig. 19. The results shown are typical, and similar results were obtained for all particle mixtures and packed bed heights. It may be seen that the density in section AB of each of the curves decreased with increasing air velocity. This was expected since more air was passing through the bed. With each increase in air velocity the density profiles became more expanded and deviated further from the ideal bed hypothesized in Fig. 14.

The effect of air velocity and height in bed upon the index of stability and uniformity is presented in Figures 20a, b, and c. The ISU profiles indicate that both the stability and uniformity decreased with increasing air velocity. This trend was characteristic of all particle mixtures.

The fact that the lower velocities were more uniform is indicated by the smaller slope of the lower portion of the ISU profiles. The better stability at lower velocities is indicated by the lower magnitude of the index. For instance, the index at three inches above the distributor was 1.5, 4.7, and 6.3 for the 30, 60, and 90 ft./min. velocities, respectively. At 6 inches above the distributor the index was 3.9, 10.2, and 12.0 for the three velocities. Results similar to this were also obtained for the other beds and are tabulated in the appendix.

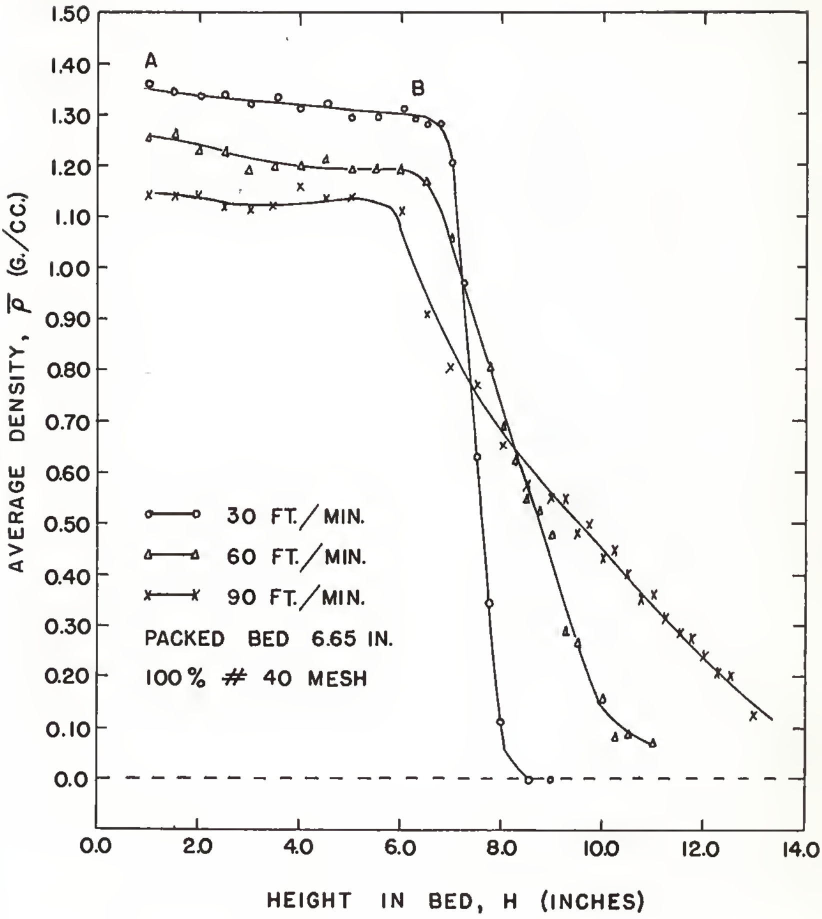

Fig. 19. Effect of air velocity upon the density profiles.

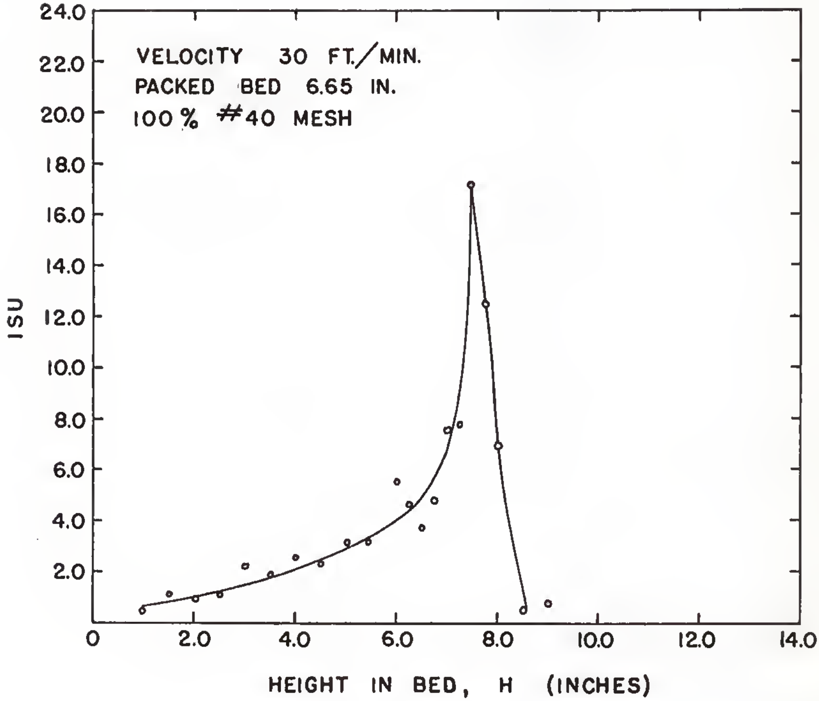

Fig. 20a. Effect of air velocity upon ISU profiles.

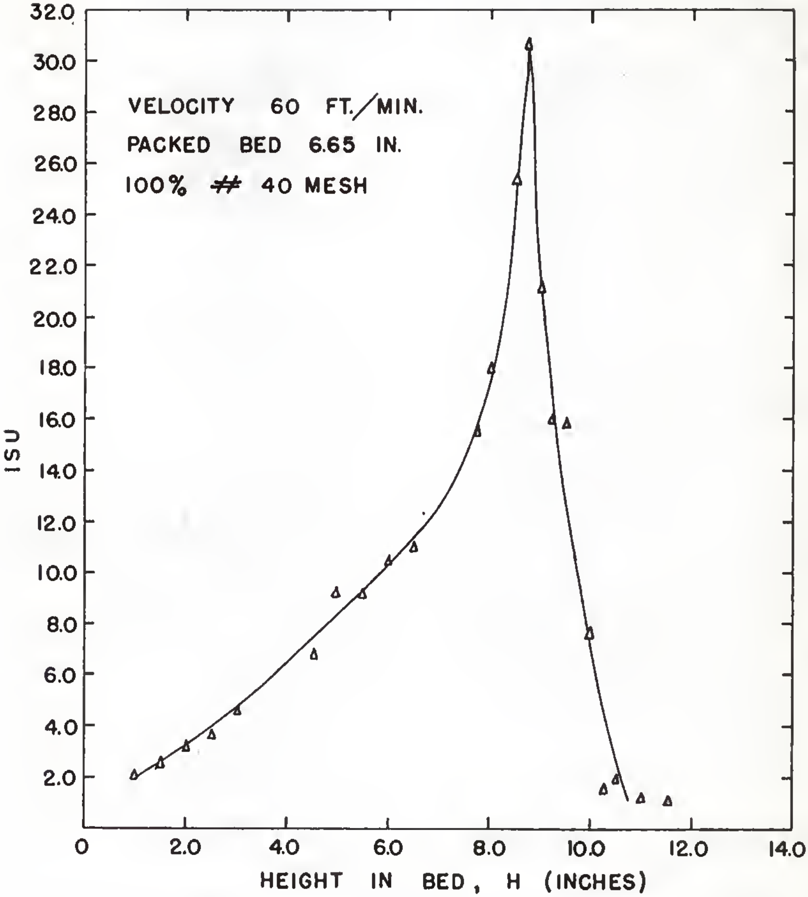

Fig. 20b. Effect of air velocity upon ISU profiles.

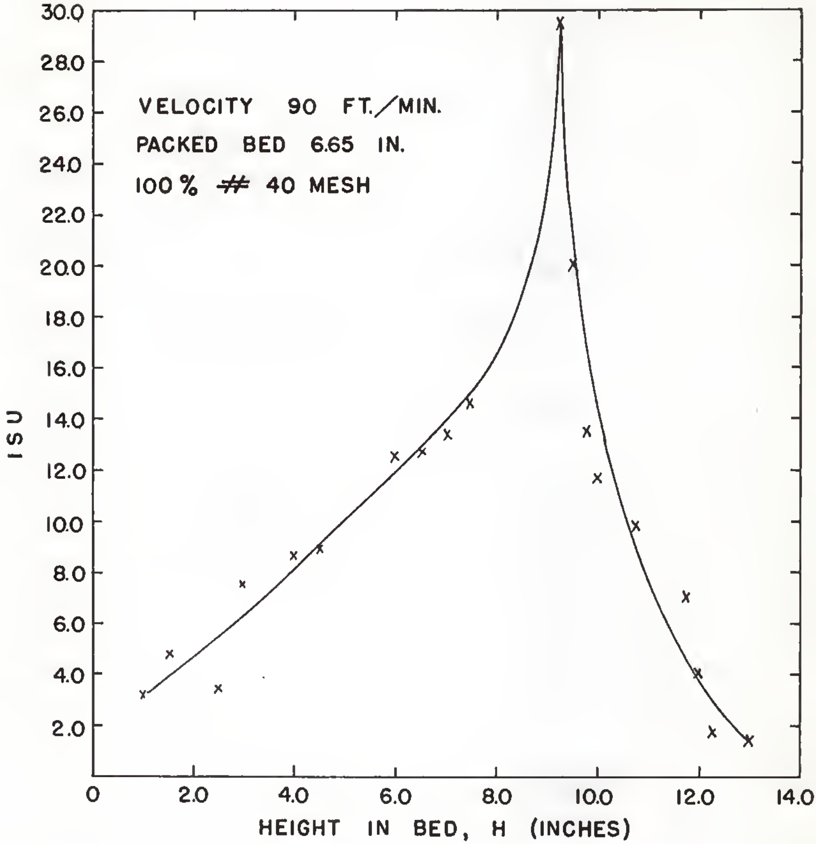

Fig. 20c. Effect of air velocity upon ISU profiles.

The index increased with increasing height above the distributor until a maximum was reached and then dropped abruptly. Aesuming that the generally accepted bubble phenomena is characteristic of the gas-solids system, this trend in the ISU indicates the following machanism which was aleo suggested by Baumgarten (1).

Ae the bubble riees, solids may be carried along with the bubble or forced out of the path of the bubble. It appears as though the rising bubble growe in size as it moves up the column, and it ie thue enabled to eupport the carriage of more solide. As the size increases, the solids mixing becomes more vigorous, and more and more solids must either be forced aside or carried along with the bubble. As the bubble approaches the eurface of the bed, the solids above it will be scattered into the empty space above the bed allowing the bubble to break the surface. The solids will then fall back to the bed. The point of maximum disturbance and instability would then be the point where the bubble breaks the surface, since at this point the eolids mixing is moet vigorous and the bubble is the largest. The epace juet above the bed is disturbed by only the scattered eolids that are thrown by the rising bubble. Density fluctuations are, therefore, relatively small above the surface.

Density Profile-ISU Profile Correlation. It was found that the shape of the density profiles could be related to the ISU profiles. It was just shown that the density profilee became more expanded and less resembled the ideal (perfectly uniform and etable) bed when the air velocity was increased. It was also shown that the stability and uniformity decreased with increasing air velocity. In every case, without exception, the density profiles and ISU profiles could be satisfactorily correlated. This suggests that it would be possible to investigate, to some extent, density fluctuations, i. e., bed quality, using a long time constant and studying only the density profile. This would remove much of the troublesome data analysis resulting from using the short time constant.

ISU and Bed Expansion. In the past there have been some problems in defining the fluidized bed height. If one tries to visually interpret the bed expansion, large discrepancies may result owing to the constant fluctuations as a result of fluidization. However, the index of stability and uniformity provides a good criterion for measuring the fluidized bed height.

It has been previously illustrated that the point where the bubbles break the surface is the point of the maximum ISU. This point would also be the fluidized bed height because this is the dense-phase surface.

Consider the ideal bed hypothesized in Fig. 14. The fluidized bed height is obviously the point where the density falls to zero. Now, applying this reasoning to the density profiles one could choose a fluidized bed height. This height, however, could be any one of several since these beds were not ideal, and the density drop to zero was over a range of two or three inches. The fluidized bed height was chosen to be the point of inflection, or the mid-point if no inflection was apparent.

Figure 21 shows a comparison of fluidized bed height using the ISU and inflection techniques. In many of the cases the two methods gave the same fluidized bed height. The greatest difference was only 0.50 inches with a 4.50-inch bed.

This analysis illustrates that the expanded bed height can very definitely be taken as the inflection point of the density profile. An even better analysis would be to use the ISU profile.

It was found that bed expansion increased with velocity as illustrated by the ISU profiles.

<u>Effect of Packed Bed Height</u>. The static bed height did not have any apparent effect upon the constant density portion of the density profile. This is illustrated in Figure 22 where the sections AB_1, AB_2, and AB_3 are approximately the same density for all three packed bed heights.

The packed bed height does affect, however, the stability and uniformity of the fluidized bed. This is readily seen in Figures 23a, b, and c which compare the ISU profiles for three packed bed heights. It is apparent that the best uniformity and stability occurred in the shallow bed. In fact, the χ^2_{39} values for the lower portion of the 3.25-inch bed profile indicated a packed bed. This may be seen in Table 14 of the appendix. The reason for the better uniformity of fluidization in the shallow bed is most probably due to the fact that bubbles have little chance to form and grow in shallow beds.

<u>Effect of Particle Size and Bed Composition</u>. Figures 24a and 241 present the vertical ISU profiles for fluidized beds of 100 percent 40 mesh and 100 percent 80 mesh at an air velocity of 30 ft./min. These profiles indicate that the finer particle

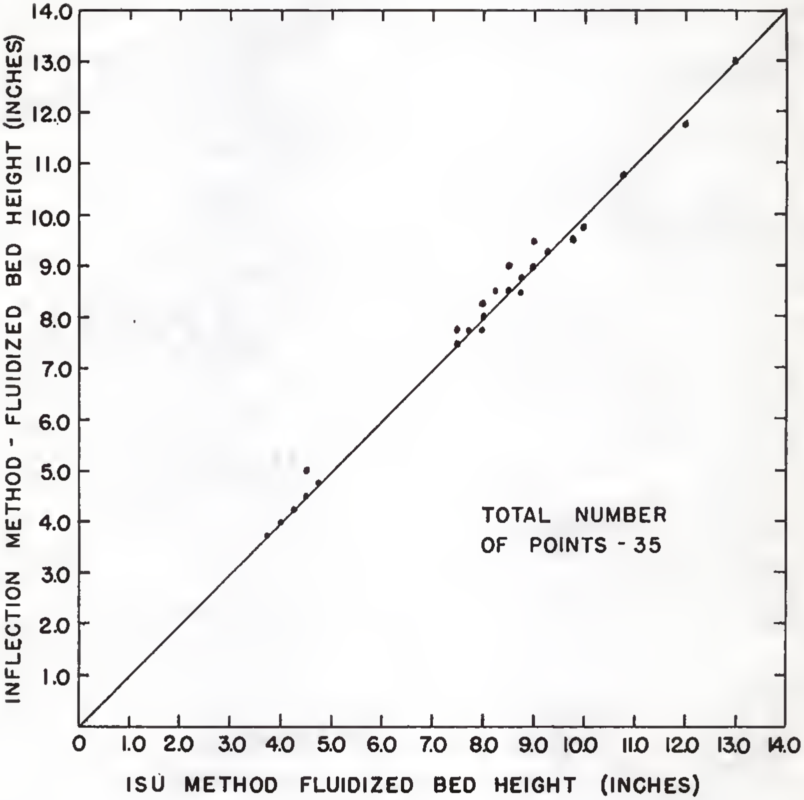

Fig. 21. Comparison of fluidized bed heights from inflection and ISU methods.

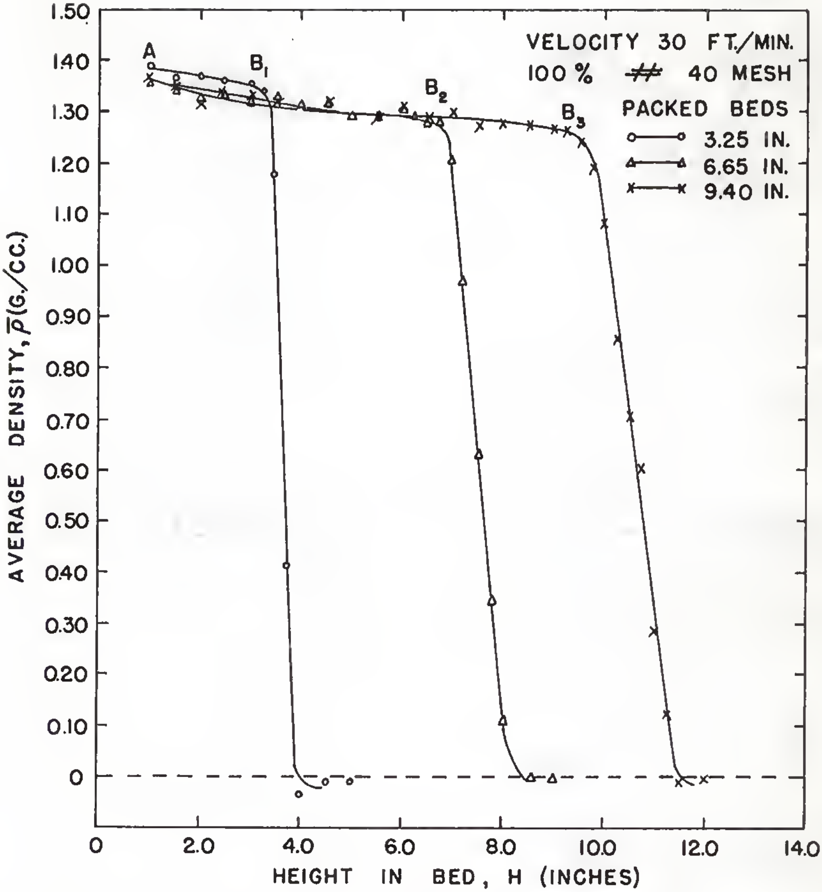

Fig. 22. Effect of packed bed height upon density profiles.

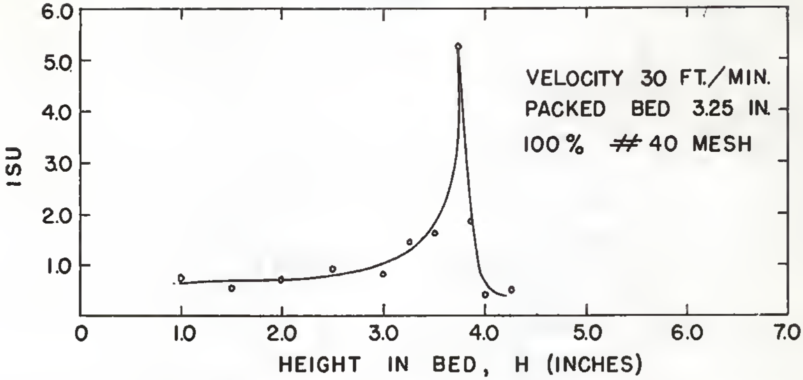

Fig. 23a. Effect of packed bed height upon ISU profiles.

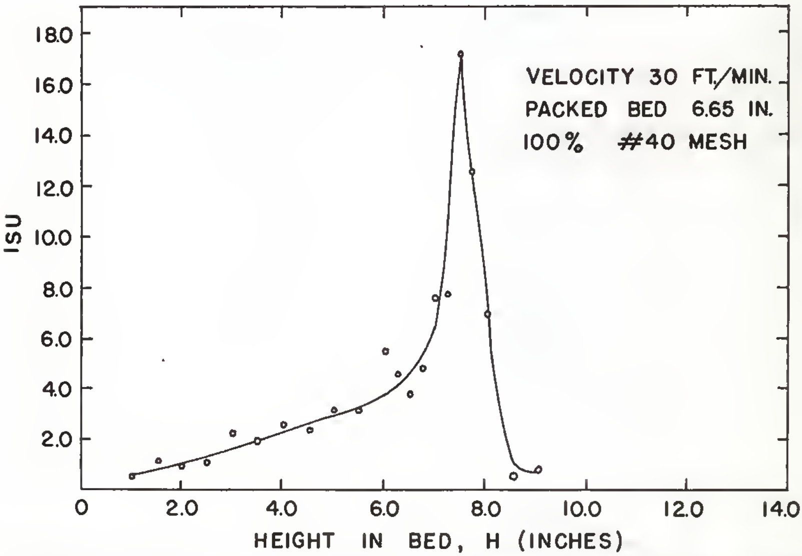

Fig. 23b. Effect of packed bed height upon ISU profiles.

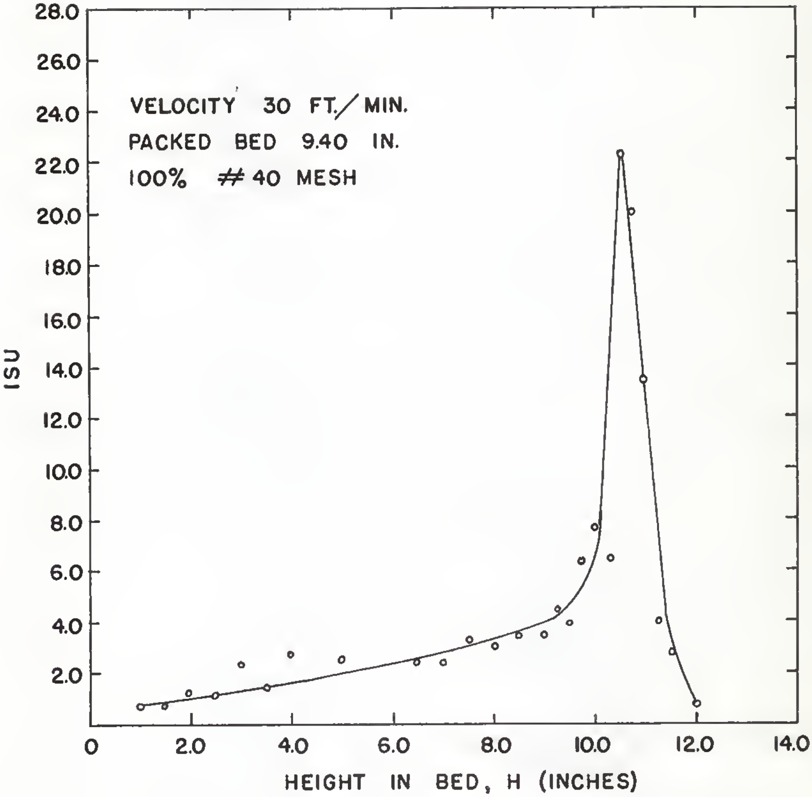

Fig. 23c. Effect of packed bed height upon ISU profiles.

size provided for both a more stable and a more uniform fluidized bed. As the velocity was increased this trend appeared to become less and in fact reversed at high velocity. For example, the ISU maxima for the 30 ft./min. velocity were 17.3 and 21.1 for the 40 mesh and 80 mesh particles, respectively. At an air velocity of 60 ft./min. the maxima were 30.7 and 30.6, and at 90 ft./min. the maxima were 29.0 and 21.2 for the 40-mesh and 80-mesh particles.

The result at the low velocity can most probably be explained by the fact that larger particles require a greater minimum fluidizing velocity (1). No bubbles at all can form until the bed is supported by the pressure drop through the interstices. This means that the bubble size will be smaller for coarse particles since a greater portion of the fluidizing gas is required for minimum fluidization.

Dotson (2) also found that coarse particles produced better uniformity of fluidization at low gas velocity; however, he attributed this trend to the presence of channeling in small particle beds which he confirmed by visual interpretation.

The reversal of the particle size effect at high velocity may be attributed to factors which oppose the minimum fluidizing effect. Increased permeability in coarse particle beds permits an increased flow of gas from the dense phase to the bubble phase, thus increasing bubble growth and the ISU. This effect becomes more important at high velocities because the amount of gas held in the dense phase is relatively constant, and at high velocities more of the gas flows into the bubble phase (14).

Reversals similar to this were also obtained by Doteon (2) and Baumgarten (1).

Figures 24a-i illustrate the effect of bed composition upón the index at low gas velocity. From these profiles it is very difficult to make any precise statement regarding bed stability and uniformity. It does appear, however, that the trend is one of relatively good stability and uniformity for particle mixtures of 100, 98, and 95 percent 40-mesh beads. The etability and uniformity appear to decrease for particle mixtures with more than 10 percent 80-mesh beads. For particle mixtures of 50 percent or more 80-meeh beads the stability and uniformity were relatively poor.

In order to better predict the effects of particle size and bed composition, it is euggested that a wider range of particle sizes be investigated.

In view of these resulte, the effect of air velocity and height in bed appear to be much more pronounced than that of particle size and bed composition. This is consistent with the findings of Dotson (2).

Channeling. It was mentioned earlier that the number of data points rejected by the 5 percent confidence test increased with air velocity. This may be explained by the increase in channeling at higher velocitiee. Leva (6) hae pointed out that very few gas-solids systems approach ideal behavior, and most are characterized by either through-channeling or intermediate-channeling, or both. When this occurs, a portion of the gas

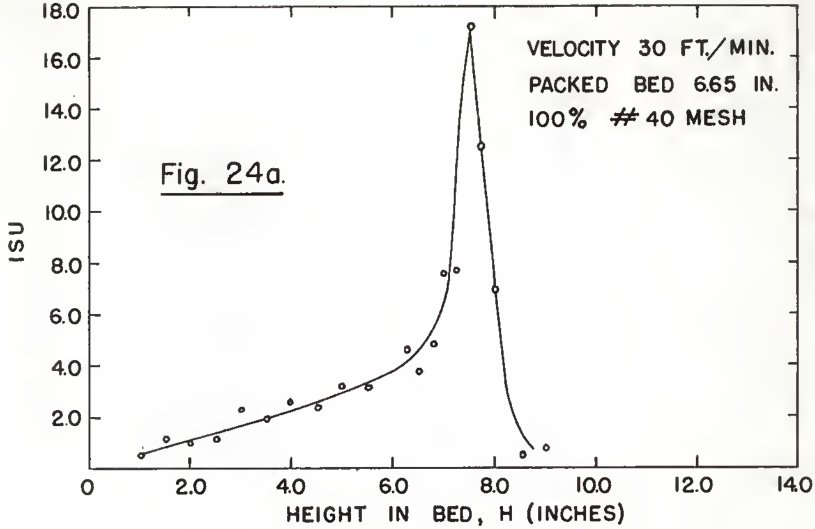

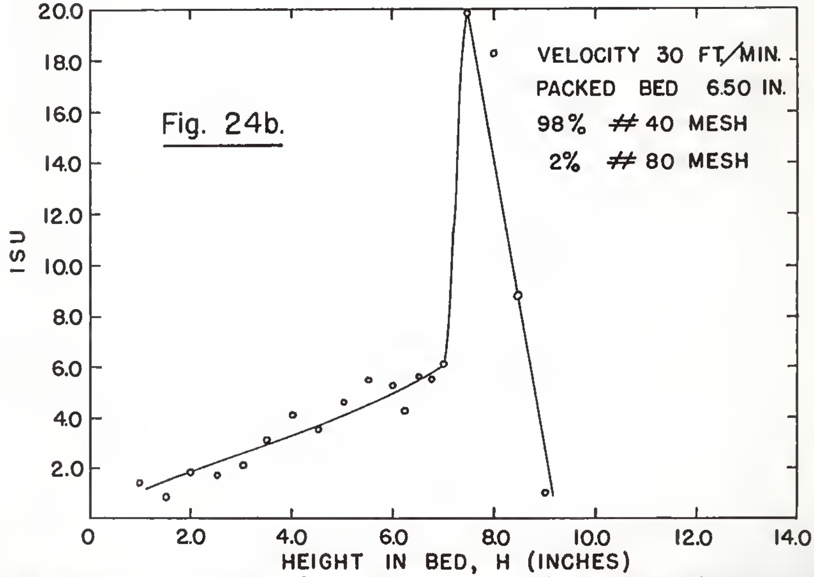

Fig. 24a,b. Effect of particle size and composition.

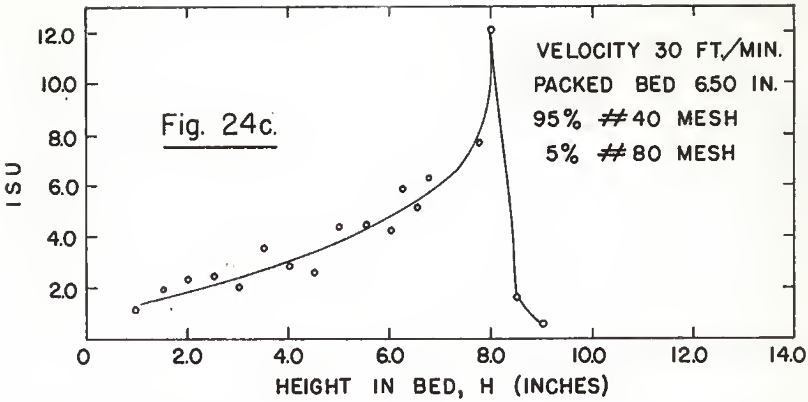

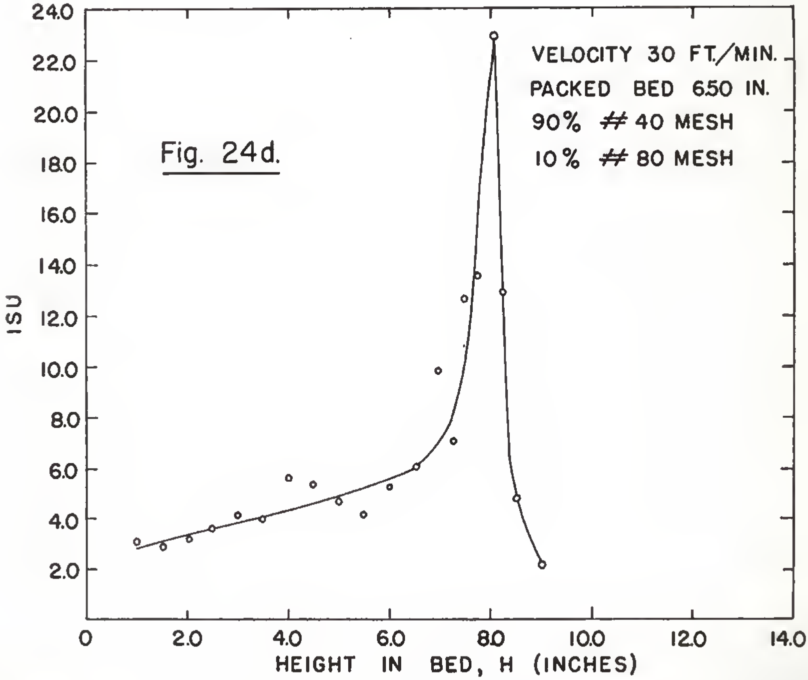

Fig. 24c,d. Effect of particle size and composition.

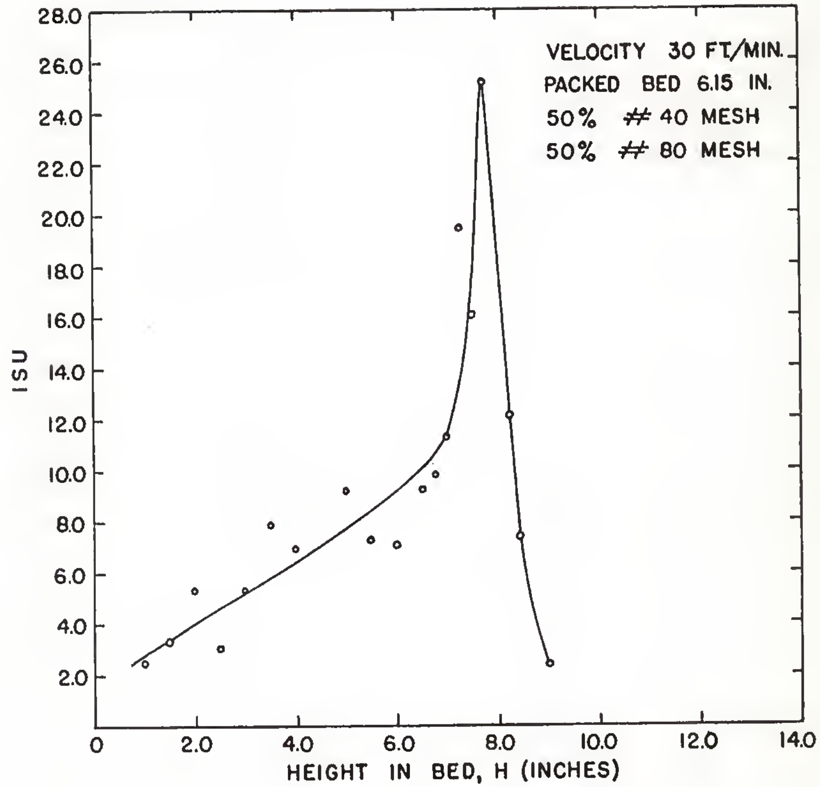

Fig. 24e. Effect of particle size and bed composition.

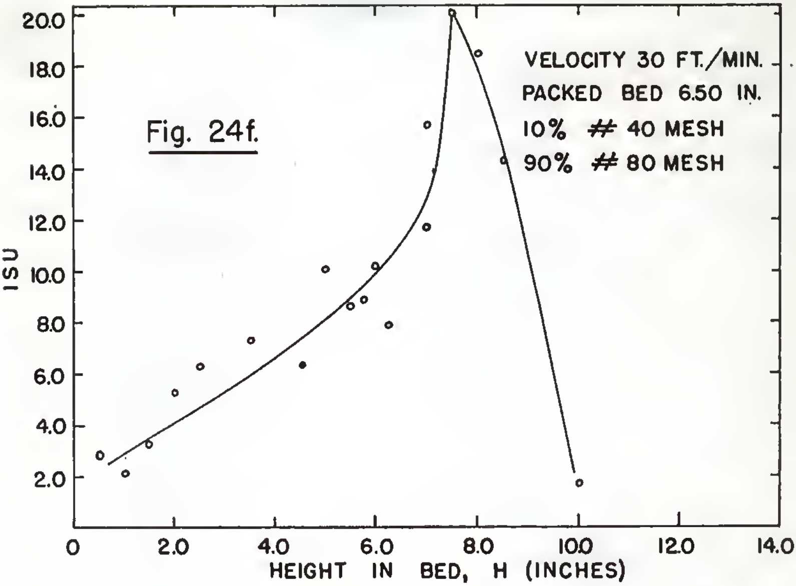

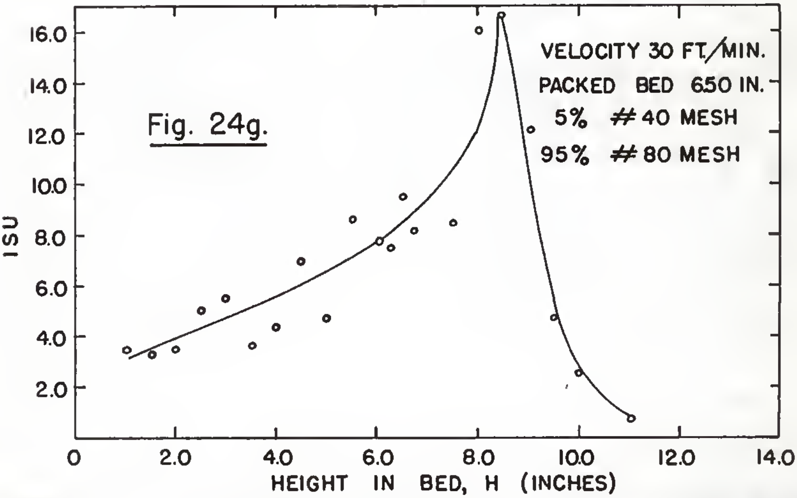

Fig. 24f,g. Effect of particle size and composition.

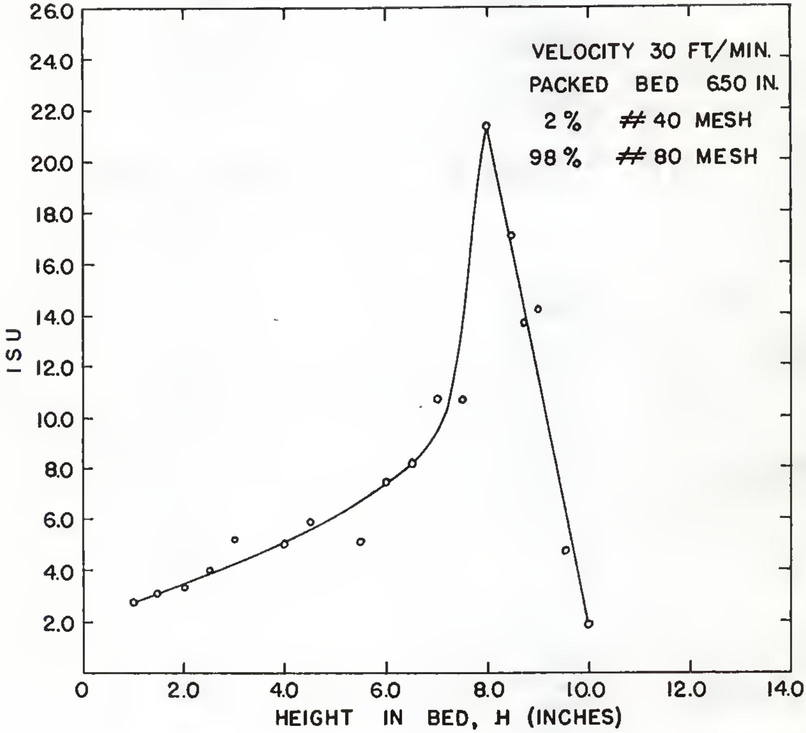

Fig. 24h. Effect of particle size and bed composition.

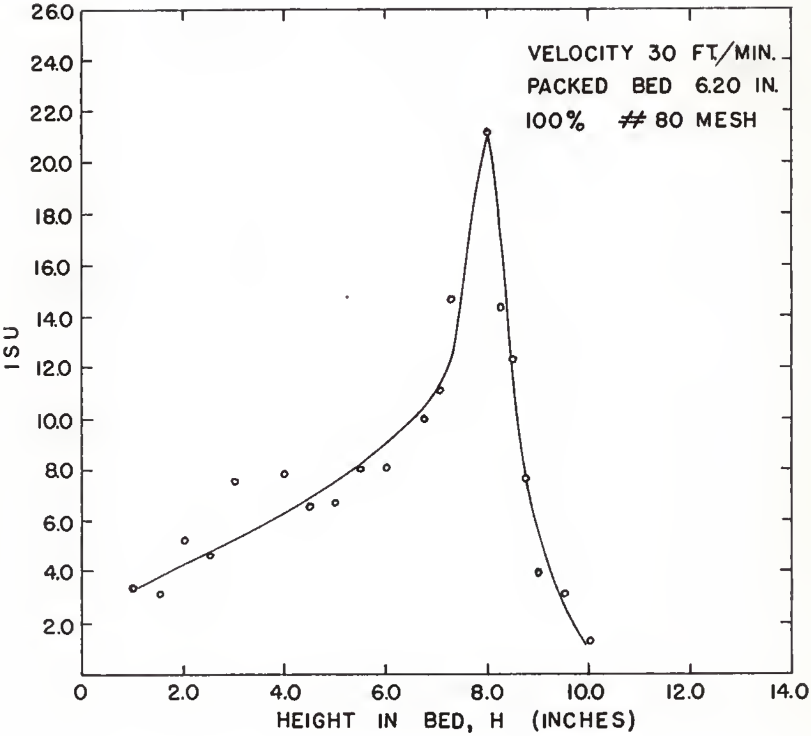

Fig. 24i. Effect of particle size and bed composition.

flow is actually piped through the bed in channels. These channels could be located anywhere in the bed. This has two undesirable effects upon the gas-solids system that has been previously described. The first effect is the addition of another phase which is neither tho bubble nor the dense phase. This now phase may be pictured as meroly the piping of gae through the bed. Thie is another form of gas by-passing the solids. This leads to the second undesirable effect. The fact that gas channels are formed moans that the by-passing is no longer completely in the form of randomly distributed bubbles. Instead, the channeling results in the flow of gas through one location in the bed. This destroys the statistical concept which is based upon randomly distributed bubbles. It may be seon in the normality test (Tablos 3-8) that the high-velocity data producod the largest valuo for g_1. Although this value of g_1 was insignificant, it was found that the channoling became apparont in some cases.

Figures 25 and 26 illustrate the effect of channeling upon the density profile and ISU profile. The constant density portion of tho density profile practically disappearod and the valuos of the index showed little or no trend whatsoever.

CONCLUSIONS

The results of this investigation have yielded the following important conclusions about gas-solids fluidized systems.

1. Using short time-constant data, the statistical approach

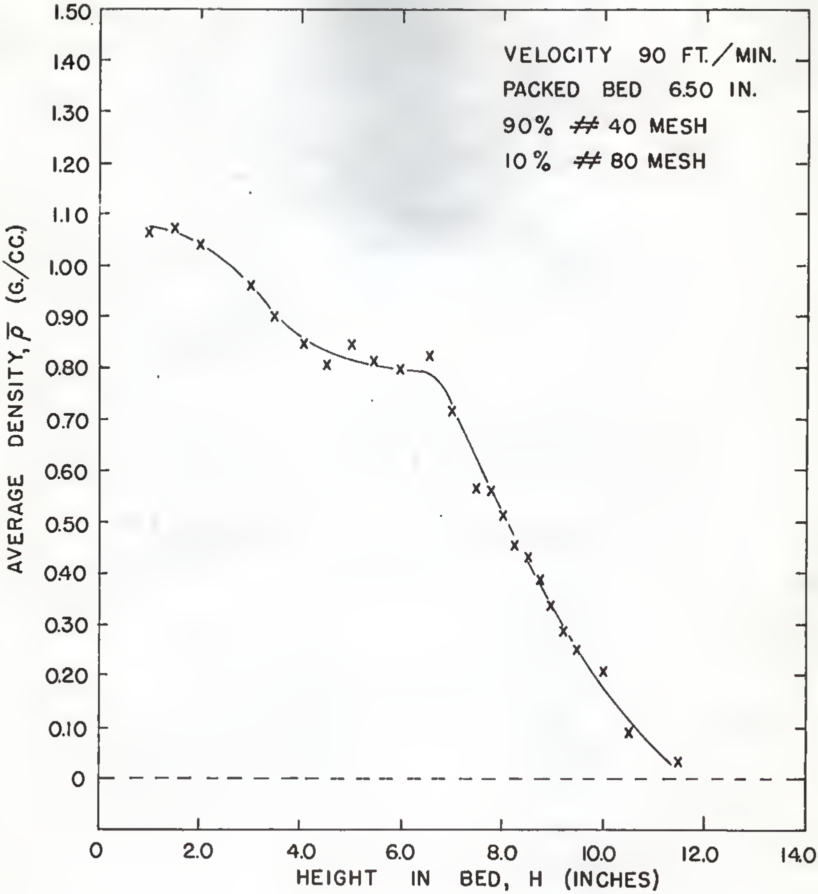

Fig. 25. Density profile when channeling is prevalent.

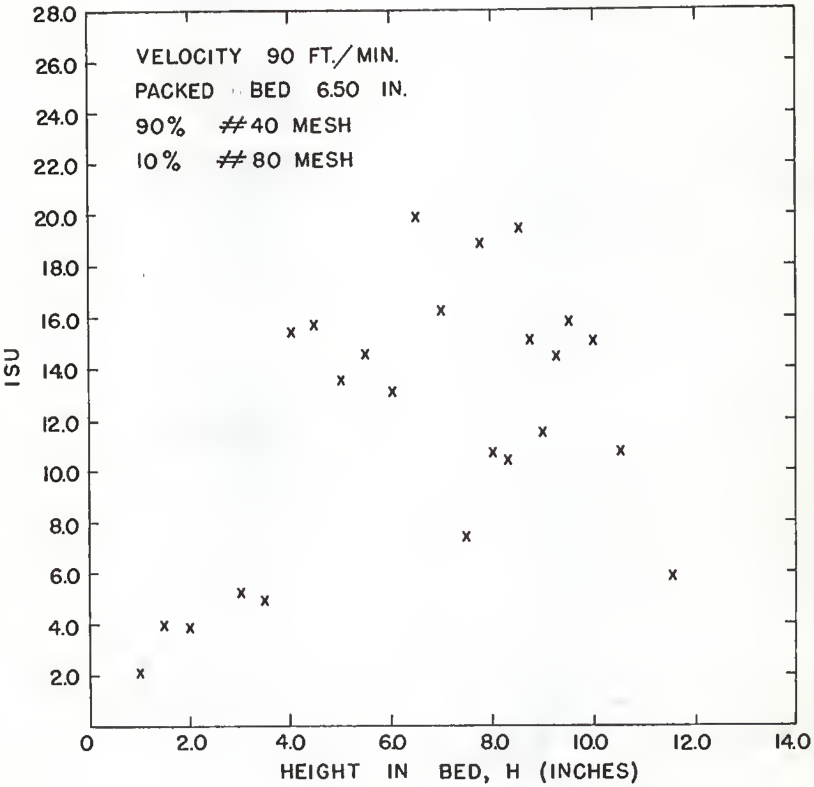

Fig. 26. Effect of channeling upon ISU.

to the study of bed quality is quite satisfactory for determining the relative effects of operational variables upon the gas-solids fluidized bed.

2. Long time-constant data may be used to a limited extent in studying bed uniformity and stability with density profiles.

3. Both stability and uniformity of fluidized beds decrease with increasing superficial gas velocity, and at high gas velocities channeling of the gas flow becomes apparent.

4. Bubbles grow in size as they move up the column and increase in size with increasing gas velocity.

5. The fluidized bed height is the point where the bubbles break the dense-phase surface and is characterized by a peak in the ISU profile. This point also corresponds to the inflection point in the vertical portion of the average density profile.

6. Static bed height does not affect the mean density of the fluidized bed; however, the mean density (constant portion of the average density profile) decreases with increasing gas velocity.

7. Shallow beds are more stable and uniform than deep beds owing to the fact that bubbles have little chance to form and then grow.

8. At low gas velocities, coarser particles produce better bed stability and uniformity. This most probably results from the fact that no bubbles can form until the bed reaches minimum fluidization, and the minimum fluidizing velocity increases with particle size. As the velocity is increased, this trend appears to reverse, and at high velocities finer particles provide better

uniformity and stability. This is probably due to the greater permeability of coarse particles which allows more bubble formation through flow of gas from the dense phase to the bubble phase.

9. The effects of gas velocity and height in the bed upon bed quality are much more pronounced than the packed bed height, particle size, and bed composition.

ACKNOWLEDGMENT

The author wishes to express his sincere appreciation to the following persons and organizations:

Dr. Liang-tseng Fan, for his constant advice and guidance throughout the course of the investigation.

Professor Richard C. Bailie, for suggesting the statistical approach using the isotope technique, for devising the original instrumentation scheme, and for directing the use of the IBM-650 Computer.

Dr. William R. Kimel, Head of the Nuclear Engineering Department at Kansas State University, for his help and encouragement.

The staffs and students of both the Nuclear Engineering and Chemical Engineering Departments for their helpful suggestions and their willingness to assist when called upon.

The Engineering Experiment Station of Kansas State University for supporting this project.

LITERATURE CITED

(1) Baumgarten, P. K.
Density fluctuation in fluidized beds. Ph. D. Thesis. University of Delaware, 1957.

(2) Dotson, J. M.
Factors affecting density transients in fluidized beds. A. I. Ch. E. J. 5:169-174. 1959.

(3) Fisher, R. A.
Statistical methods for research workers. 6th ed. London: Oliver and Boyd, 1936.

(4) Groshe, E. W.
Analysis of gas-fluidized solid systems by X-ray absorption. A. I. Ch. E. J. 1:358-365. 1955.

(5) Lee, C. J.
Unpublished thesis. Kansas State University, 1961.

(6) Leva, Max.
Fluidization. New York: McGraw-Hill, 1959.

(7) Lindley, D. V., and J. C. P. Miller.
Cambridge elementary statistical tables. Cambridge: Cambridge University Press, 1953.

(8) Morse, R. D., and C. O. Ballou.
The uniformity of fluidization - its measurement and use. Chem. Eng. Prog. 47(4):199-204. 1951.

(9) Othmer, Donald F.
Fluidization. New York: Reinhold, 1956.

(10) Petrick, M. and B. S. Swanson.
Radiation attenuation method of measuring density of a two-phase fluid. Rev. Sci. Instruments. 29(12):1079-1085. December, 1958.

(11) Romero, J. B.
Factors affecting fluidized bed quality. Ph. D. Thesis. University of Washington, 1959.

(12) Shuster, W. W., and P. Kisliak.
The measurement of fluidization quality. Chem. Eng. Prog. 48(9):455-458. 1952.

(13) Snedecor, George W.
Statistical methods. 4th ed. Ames: Iowa State College Press, 1946.

(14) Zenz, F. A., and D. F. Othmer.
Fluidization and fluid - particle systems. New York:
Reinhold, 1956.

LIST OF SYMBOLS

A - variance intercept of linear regression.

B - slope of line in linear regression.

d - thickness of absorber, cm.

F - variance ratio of the F-test.

g - g-statistic.

H - height in bed (above distributor), inches.

I/I_o - fraction of photons remaining in the beam after passage through absorber of thickness d.

ISU - index of stability and uniformity.

k - k-statistic.

m - median of the variate x_i.

M - atomic weight, g./g-mol.

N - number of observational data

N_a - Avagodro's number (6.025×10^{23} nuclei/g-mol.).

P - probability.

R - width for the beam path, inches.

s - sums of powers of the variate x_i.

S - sums of powers of the deviations in x_i from the mean $\bar{x}$.

x_i - variate.

$\bar{x}$ - mean (average) value of the variate x_i.

y - criterion for the significance of the test for normality.

LIST OF SYMBOLS (cont.)

Greek letters.

γ - gamma radiation.

μ - linear absorption coefficient, cm^{-1}.

ν - degrees of freedom.

ρ - density, g./cc.

$\bar{\rho}$ - average density, g./cc.

σ - standard deviation (estimate of).

σ^2 - variance.

σ^* - standard error in sampling.

σ^{*2} - sampling variance.

σ - microscopic cross section, cm^2./nucleus.

χ^2 - chi-square test for goodness of fit.

Subscripts.

c - column.

f - fluidized.

g - g-statistic.

p - packed.

s - spacer.

x - variate x_i.

1,2,3,4, - refer to different statistics such as s_1, g_2, k_3, etc.

ν - degrees of freedom.

APPENDIX

Description and Explanation of IBM-650 Computer Program for the Statistical Analysis

The IBM-650 code for the statistical analysis was written in SOAP II form. The SOAP output and a logic diagram of the program are presentod at the end of this section.

Program. The program was written to give the following important quantities from the forty densities of the fluidized bed recorder trace:

1. code number,
2. number of experimental data points, N,
3. highest density, $\rho_{max.}$,
4. lowest density, $\rho_{min.}$,
5. average density, $\bar{\rho}$,
6. variance in density of the fluidized bed, σ_f^2,
7. variance for the packed bed of similar density, σ_p^2,
8. variance ratio, index of stability and uniformity, ISU,
9. sum of the squares of the deviations from the mean, S_2,

and

10. chi-square, χ^2.

Equations used for the calculation of $\bar{\rho}$, σ_f^2, σ_p^2, ISU, S_2, and χ^2 were (1), (3), (6), (5), (2), and (4) respectively.

The code number was used for keeping track of the experiments, i. e., run number, particle size, velocity, height in bed at which the data were taken. The highest and lowest values of density were useful in finding mistakes in data card punching. The number of data points was also quite useful in checking unusual results. The highest value, lowest value, and number of data points made it relatively easy to find most program errors.

Symbolic Representation. The symbols corresponding to terms in the equations are listed below.

A - the constant, A, in the linear regression, equation (6).

B - the constant, B, in the linear regression, equation (6).

CHISQ - chi-square, χ^2.

CODE - code number.

DSQDF - standard deviation squared (variance) of the fluidized bed, σ_f^2.

DSQDP - standard deviation squared (variance) of the packed bed, σ_p^2.

HIGH - highest density in a given set of data.

LOW - lowest density in a given set of data.

N - number of data points.

RATIO - variance ratio, ISU.

SX - sum of the x terms, s_1.

SXSQ - sum of the x^2 terms, s_2.

TEMP1 - sum of deviations squared, S_2.

TEMP2 - degrees of freedom, N-1.

X - density (data point), ρ.

XAVG - average density, $\bar{\rho}$.

Input Data. A set of input data, consisting of a code number and forty densities was fed into the machine in the following manner. The code number and data points were put on IBM cards at eight words to a card. The first word on the first card was the code number. The remaining seven words on the first card were data points. The second, third, fourth, and fifth cards each contained eight data points making a total of thirty-nine data points. The final data point was punched as the first word on the sixth card, the remaining seven words being punched zero. Other sets of data followed directly after the first set with six cards to each set.

Each set of data was coded in the following manner. The code number, as the rest of the words, had ten digits. The first two digits were used for the run number, the next three for the percent of 40-mesh particles, the next for the velocity, and the final four for the height in the bed at which the data were taken. In general the sets of data for one complete vertical traverse, i. e., one complete run, were grouped together. A transfer card was placed between the program deck and the data cards to start the program.

Output Data. The computer calculations yielded ten answers for each set of data. These were punched on two cards. The first card contained eight answers in the following order: CODE, N, HIGH, LOW, XAVG, DSQDF, DSQDP, and RATIO. The second card also contained eight answers, six of which were repeated from the first card. The answers were CODE, N, HIGH, LOW, XAVG, TEMP1, DSQDP, and CHISQ. When more than one set of data were analyzed, the answer cards were always punched in order, i. e., set 1, cards 1 and 2; set 2, cards 1 and 2; etc.

Console Settings for Operation. The following console settings were used:

Storage Entry Switches - 70 1951 1999 +

Programmed Stop - STOP

Half Cycle - RUN

Control - RUN

Address Selection - Anything

Display - Anything

Overflow - STOP

Error - STOP

SOAP II OUTPUT FOR THE STATISTICAL ANALYSIS

```
          BLR  1951     1958    READ            1    0000    00  0000  0000
          BLR  1977     1984    PRINT           2    0000    00  0000  0000
          BLR  0800     0900    TRACE           3    0000    00  0000  0000
          BLR  1000     1500    DATA            4    0000    00  0000  0000
          SYN  CODE     1000                    5    0000    00  0000  0000
          SYN  X        1000                    6    0000    00  0000  00 0
          SYN  START    1999                    7    0000    00  0000  [illegible]
          SYN  SHIFT    0500                    8    0000    00  0000  [illegible]
ZERO      00   0000     0000                    9    0000    00  0000  0000
100       10   0000     0053                   10    0050    10  0000  0053
SIXTY     00   0000     0060                   11    0100    00  0000  0060
ONE       10   0000     0051                   12    0150    10  0000  0051
A         38   1227     8947                   13    0200    38  1227  8947
B         49   1465     8447                   14    0250    49  1465  8447
START     RAA  0000     CONT3                  15    1999    80  0000  0005
CONT3     RCD  1951             LOAD DATA      16    0005    70  1951  0001
          LDD  1951             IN             17    0001    69  1951  0004
          STO  X      A         LOCATIONS      18    0004    24  3000  0003
          AXA  0001             STARTING       19    0003    50  0001  0009
          LDD  1952             WITH           20    0009    69  1952  0055
          STO  X      A         1001           21    0055    24  3000  0053
          AXA  0001                            22    0053    50  0001  0059
          LDD  1953             CODE NUMB      23    0059    69  1953  0006
          STO  X      A         IS             24    0006    24  3000  0103
          AXA  0001             LOCATED        25    0103    50  0001  0109
          LDD  1954             IN             26    0109    69  1954  0007
          STD  X      A         1000           27    0007    24  3000  0153
          AXA  0001                            28    0153    50  0001  0159
          LDD  1955                            29    0159    69  1955  0008
          STO  X      A                        30    0008    24  3000  0203
          AXA  0001                            31    0203    50  0001  0209
          LDD  1956                            32    0209    69  1956  0259
          STO  X      A                        33    0259    24  3000  0253
          AXA  0001                            34    0253    50  0001  0309
          LDD  1957                            35    0309    69  1957  0010
          STO  X      A                        36    0010    24  3000  0303
          AXA  0001                            37    0303    50  0001  0359
          LDD  1958                            30    0359    69  1958  0011
          STO  X      A                        39    0011    24  3000  0353
          RAU  8001                            40    0353    60  8001  0061
          NZE  CONT1    CONT2                  41    0061    45  0014  0015
CONT1     AXA  0001     CONT3                  42    0014    50  0001  0005
CONT2     SXA  0001                            43    0015    51  0001  0021
          RAU  X      A                        44    0021    60  3000  0105
          NZE  CONT4    CONT2                  45    0105    45  0058  0015
CONT4     LDD  8005                            46    0058    69  8005  0064
          STO  N                NO OF PTS      47    0064    24  0017  0020
          LDD  ZERO                            48    0020    69  0000  0403
          STO  HIGH                            49    0403    24  0056  0409
          STO  SX                              50    0409    24  0012  0065
          STO  SXSQ     CONT5                  51    0065    24  0018  0071
CONT5     RAU  SX                              52    0071    60  0012  0067
          FAD  X      A         FORM SUM       53    0067    32  3000  0027
          STU. SX               OF             54    0027    21  0012  0115
          SXA  0001             X TERMS        55    0115    51  0001  0121
          NZA  CONT5    CONT6                  56    0121    40  0071  0025
CONT6     LDD  N                SET IRA        57    0025    69  0017  0070
          RAA  8001     CONT7   TO N           58    0070    80  8001  0026
CONT7     RAU  X      A                        59    0026    60  3000  0155
          FMP  X      A         FORM SUM       60    0155    39  3000  0300
          FAD  SXSQ             OF X           61    0300    32  0018  0045
          STU  SXSQ             SQD            62    0045    21  0018  0171
          SXA  0001             TERMS          63    0171    51  0001  0077
          NZA  CONT7    CONT8                  64    0077    40  0026  0031
```

```
CONT8   LDD  N                  SET IRA TO    65   .0031   69 0017 0120
        RAA   8001     CON11    N             66    0120   80 8001 0076
CON11   RAU  HIGN               FIND          67    0076   60 0056 0111
        FSB  X        A         NIGHEST X     68    0111   33 3000 0127
        BMI  CONT9     CON10    VALUE         69    0127   46 0030 0081
CONT9   LDD  X        A                       70    0030   69 3000 0453
        STD  HIGN    .  CON10                 71    0453   24 0056 0081
CON10   SXA   0001                            72    0081   51 0001 0037
        NZA  CON11     CON12                  73    0037   40 0076 0041
CON12   LDD  N                                74    0041   69 0017 0170
        RAA   8001                            75    0170   80 8001 0126
        LDD  100                FIND          76    0126   69 0050 0503
        STD  LOW       CON15    LOWEST        77    0503   24 0106 0459
CON15   RAU  LOW                VALUE OF      78    0459   60 0106 0161
        FSB  X        A         X             79    0161   33 3000 0177
        BMI  CON13     CON14                  80    0177   46 0080 0131
CON14   LDD  X        A                       81    0131   69 3000 0553
        STD  LOW     .  CON13                 82    0553   24 0106 0080
CON13   SXA   0001                            83    0080   51 0001 0036
        NZA  CON15     CON16                  84    0036   40 0459 0040
CON16   RAU  N                  CONVERT N     85    0040   60 0017 0221
        SCT  SHIFT              TO FLOAT      86    0221   36 0500 0043
        SUP   8002              POINT         87    0043   11 8002 0051
        AUP  SIXTY                            88    0051   10 0100 0205
        STU  N                                89    0205   21 0017 0220
        RSU  SX                 FORM SUM      90    0220   61 0012 0117
        FMP  SX                 OF            91    0117   39 0012 0062
        FDV  N                  DEVIATIONS    92    0062   34 0017 0167
        FAD  SXSD               SQD           93    0167 . 32 0018 0095
        STU  TEMP1                            94    0095   21 0350 0603
        RAU  N                  FORM          95    0603   60 0017 0271
        FSB  ONE                DEGREES OF    96    0271   33 0150 0227
        STU  TEMP2              FREEDOM       97    0227   21 0032 0035
        RAU  TEMP1                            98    0035   60 0350 0255
        FDV  TEMP2                            99    0255   34 0032 0082
        STU  DSDOF              VARIANCE     100    0082   21 0086 0039
        RAU  SX                 FLUIDIZED    101    0039   60 0012 0217
        FDV  N                               102    0217   34 0017 0267
        STU  XAVG               AVG X VAL    103    0267   21 0022 0075
        RAU  XAVG                            104    0075   60 0022 0277
        FMP  B                  VARIANCE     105    0277   39 0250 0400
        FAD  A                  PACKEO       106    0400   32 0200 0327
        STU  DSDDP                           107    0327   21 0132 0085
        RAU  DSDDF              VARIANCE     108    0085   60 0086 0091
        FDV  DSQDP              RATIO        109    0091   34 0132 0182
        STU  RATIO                           110    0182   21 0136 0089
        RAU  TEMP1                           111    0089   60 0350 0305
        FDV  DSQDP              CNI SOUANE   112    0305   34 0132 0232
        STU  CNISD                           113    0232   21 0186 0139
        LDD  CODE                            114    0139   69 1000 0653
        STD   1977                           115    0653   24 1977 0130
        LDD  N                               116    0130   69 0017 0270
        STD   1978                           117    0270   24 1978 0181
        LDD  HIGH                            118    0181   69 0056 0509
        STD   1979                           119    0509   24 1979 0282
        LDD  LOW                             120    0282   69 0106 0559
        STD   1980                           121    0559   24 1980 0033
        LDD  XAVG                            122    0033   69 0022 0125
        STD   1981                           123    0125   24 1981 0034
        LDD  DSQDF              PUNCH DATA   124    0034   69 0086 0189
        STD   1982                           125    0189   24 1982 0135
        LDD  DSDDP                           126    0135   69 0132 0185
        STD   1983                           127    0185   24 1983 0236
        LDD  RATIO                           128    0236   69 0136 0239
        STD   1984                           129    0239   24 1984 0087
        PCH   1977     CDPCN                 130    0087   71 1977 0377
CDPCN   LDD  TEMP1                           131    0377   69 0350 0703
        STD   1982                           132    0703   24 1982 0235
        LDD  CHISD                           133    0235   69 0186 0289
        STD   1984                           134    0289   24 1984 0137
        PCH   1977     START                 135    0137   71 1977 1999
```

LOGIC DIAGAM far IBM 650 PROGRAM

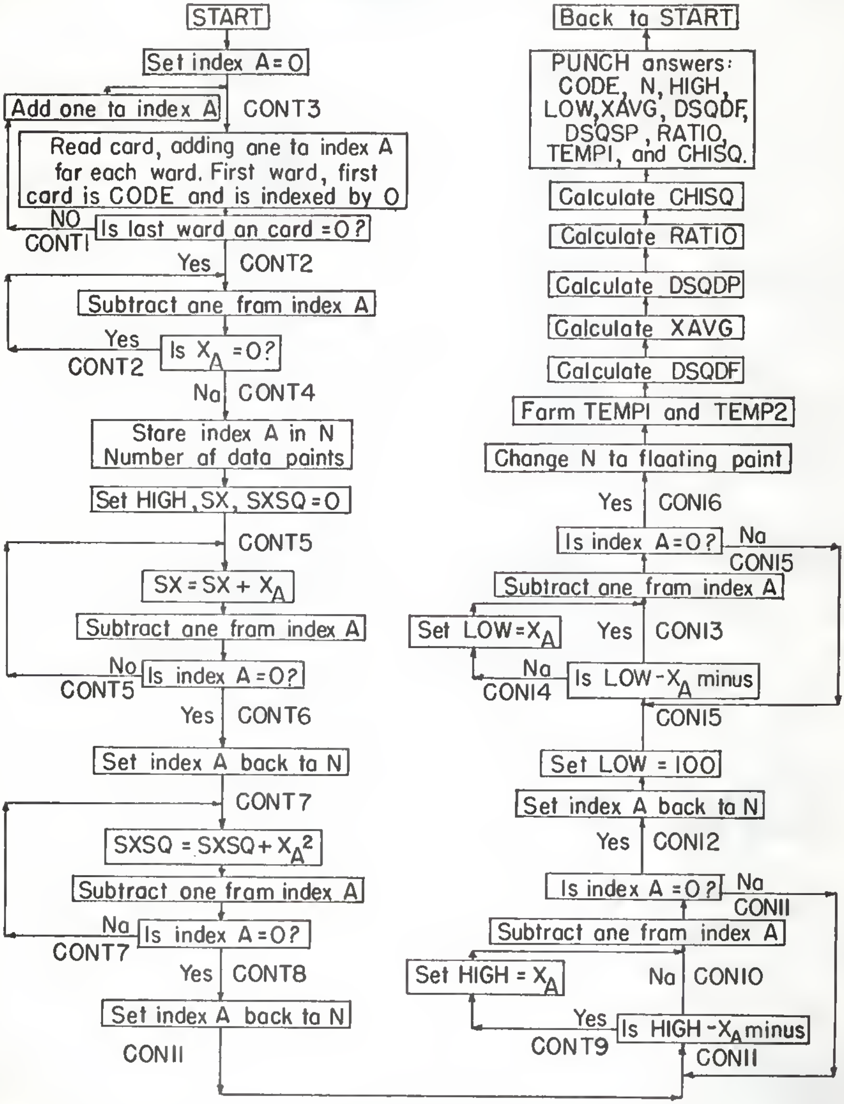

Tables

Table 9. Reduced data for run #1.

Packed bed height: 6.65 in.	Air velocity: 30 ft./min.	Particle size:	100% 40 mesh, 0% 80 mesh.
H inches	$\bar{\rho}$ g./cc.	ISU	χ^2_{39}
1.00	1.360	0.58	22.80
1.50	1.345	1.02	39.82
2.00	1.332	0.96	37.68
2.50	1.336	1.03	40.25
3.00	1.321	2.23	87.15
3.50	1.333	1.91	74.68
4.00	1.311	2.47	96.40
4.50	1.320	2.39	93.31
5.00	1.295	3.16	123.47
5.50	1.291	3.10	121.14
6.00	1.316	5.52	215.39
6.25	1.293	4.45	173.79
6.50	1.281	3.67	143.19
6.75	1.285	4.80	187.56
7.00	1.206	7.47	291.69
7.25	0.966	7.60	296.44
7.50	0.637	17.26	673.42
7.75	0.342	12.54	489.38
8.00	0.113	6.96	271.47
8.50	0.093	0.46	18.07
9.00	0.030	0.72	28.22

Table 10. Reduced data for run #2.

Packed bed height: 6.65 in.	Air velocity: 60 ft./min.	Particle size:	100% 40 mesh, 0% 80 mesh.
H inches	$\bar{\rho}$ g./cc.	ISU	χ^2_{39}
1.00	1.250	2.03	79.22
1.50	1.264	2.52	98.54
2.00	1.230	3.36	131.23
2.50	1.228	3.69	144.01
3.00	1.196	4.68	182.61
3.50	1.204	7.72	301.14
4.00	1.184	7.70	300.35
4.50	1.218	6.41	250.17

Table 10 (concl.).

H inches	$\bar{\rho}$ g./cc.	ISU	χ^2_{39}
5.00	1.196	9.17	357.64
5.50	1.192	9.00	351.24
6.00	1.191	10.47	408.37
6.50	1.174	11.06	431.56
7.00	1.063	7.71	300.81
7.50	0.967	9.32	363.78
7.75	0.812	9.79	381.91
8.00	0.691	15.53	605.98
8.25	0.632	18.26	712.30
8.50	0.555	25.39	990.28
8.75	0.533	30.66	1195.97
9.00	0.467	21.16	825.43
9.25	0.298	16.16	630.53
9.50	0.272	15.91	620.79
10.00	0.161	7.54	294.29
10.25	0.089	1.44	56.35
10.50	0.094	1.97	77.13
11.00	0.076	1.16	45.39
11.50	0.073	1.00	39.32
12.00	0.064	1.33	51.88

Table 11. Reduced data for run #3.

Packed bed height; 6.65 in. Air velocity: 90 ft./min. Particle size: 100% 40 mesh, 0% 80 mesh.

H inches	$\bar{\rho}$ g./cc.	ISU	χ^2_{39}
1.00	1.144	3.16	123.26
1.50	1.147	4.87	190.23
2.00	1.145	9.60	374.63
2.50	1.123	3.55	138.50
3.00	1.115	7.49	292.17
3.50	1.120	11.76	458.89
4.00	1.169	8.49	331.42
4.50	1.138	8.92	348.07
5.00	1.138	15.37	599.61
5.50	1.129	12.60	491.67
6.00	1.114	12.27	478.79
6.50	0.903	12.61	492.12
7.00	0.809	13.38	521.88
7.50	0.773	14.52	566.39

Table 11. (concl.).

H inches	$\bar{\rho}$ g./cc.	ISU	χ^2_{39}
8.00	0.652	7.98	311.27
8.50	0.575	12.10	472.20
9.00	0.557	13.82	539.33
9.25	0.556	29.00	113.13
9.50	0.480	20.24	789.48
9.75	0.505	13.59	530.04
10.00	0.432	11.79	460.12
10.25	0.451	19.13	746.37
10.50	0.407	25.01	975.42
10.75	0.354	9.89	385.80
11.00	0.365	12.31	480.47
11.25	0.318	6.85	267.37
11.50	0.283	11.33	441.89
11.75	0.273	7.23	282.15
12.00	0.237	4.01	156.42
12.25	0.205	1.69	65.97
12.50	0.209	1.84	71.78
13.00	0.116	1.21	47.38

Table 12. Reduced data for run #4.

Packed bed height; 9.40 in.	Air velocity: 30 ft./min.	Particle size:	100% 40 mesh, 0% 80 mesh.
H inches	**$\bar{\rho}$ g./cc.**	**ISU**	**χ^2_{39}**
1.00	1.371	0.87	34.14
1.50	1.343	0.80	31.23
2.00	1.315	1.38	54.09
2.50	1.336	1.26	49.44
3.00	1.335	2.44	95.52
3.50	1.322	1.55	60.77
4.00	1.296	2.96	115.47
4.50	1.321	3.99	155.75
5.00	1.312	2.47	96.65
5.50	1.297	4.07	159.05
6.00	1.312	4.53	177.03
6.50	1.282	2.58	100.86
7.00	1.301	2.43	95.08
7.50	1.276	3.42	133.46
8.00	1.287	3.16	123.30
8.50	1.289	3.52	137.66

Table 12. (concl.).

H inches	$\bar{\rho}$ g./cc.	ISU	χ^2_{39}
9.00	1.275	3.69	143.93
9.25	1.261	4.41	172.24
9.50	1.248	4.06	158.69
9.75	1.191	6.45	251.55
10.00	1.095	7.87	307.06
10.25	0.859	6.38	249.17
10.50	0.704	22.21	866.27
10.75	0.605	20.30	791.73
11.00	0.288	13.57	529.57
11.25	0.132	4.07	158.82
11.50	0.038	3.46	135.17
12.00	-0.003	0.87	34.28

Table 13. Reduced data for run #5.

Packed bed height: 9.40 in. Air velocity: 60 ft./min. Particle size: 100% 40 mesh, 0% 80 mesh.

H inches	$\bar{\rho}$ g./cc.	ISU	χ^2_{39}
1.00	1.237	1.67	65.47
1.50	1.252	3.22	125.89
2.00	1.214	3.33	130.01
2.50	1.193	7.92	309.20
3.00	1.189	7.12	277.75
3.50	1.189	6.76	263.98
4.00	1.197	3.47	135.56
4.50	1.141	11.85	462.38
5.00	1.215	9.98	337.77
5.50	1.170	10.41	406.09
6.00	1.186	9.35	364.69
6.50	1.129	9.99	389.84
7.00	1.133	17.88	697.34
7.50	1.117	8.60	335.42
8.00	1.144	13.48	526.06
8.50	1.146	12.08	471.40
9.00	1.093	10.36	404.38
9.50	1.057	13.38	521.85
10.00	0.858	17.33	676.22
10.25	0.856	12.51	488.08
10.50	0.847	18.03	703.49
10.75	0.787	16.65	649.58

Table 13. (concl.).

H inches	$\bar{\rho}$ g./cc.	ISU	χ^2_{39}
11.00	0.747	11.32	441.77
11.25	0.749	16.34	637.55
11.50	0.730	18.65	727.36
11.75	0.708	17.14	668.84
12.00	0.661	23.09	900.56
12.25	0.598	25.86	1008.60
12.50	0.510	38.33	1495.02
12.75	0.481	30.85	1203.30
13.00	0.409	39.40	1536.83

Table 14. Reduced data for run #6.

Packed bed height: 3.25 in. Air velocity: 30 ft./min. Particle size: 100% 40 mesh, 0% 80 mesh.

H inches	$\bar{\rho}$ g./cc.	ISU	χ^2_{39}
1.00	1.390	0.768	29.96
1.50	1.369	0.583	22.76
2.00	1.368	0.734	28.64
2.50	1.366	0.921	35.94
3.00	1.356	0.855	33.37
3.25	1.345	1.427	55.65
3.50	1.172	1.621	63.24
3.75	0.419	5.220	203.59
4.00	0.049	1.888	73.64
4.50	-0.004	0.414	16.18
5.00	-0.006	0.517	20.16

Table 15. Reduced data for run #7.

Packed bed height: 3.25 in.	Air velocity: 60 ft./min.	Particle size:	100% 40 mesh, 0% 80 mesh.
H inches	$\bar{\rho}$ g./cc.	ISU	χ^2_{39}
1.00	1.240	1.39	54.41
1.50	1.236	3.24	126.60
2.00	1.248	2.43	94.77
2.50	1.271	1.45	56.59
3.00	1.267	2.52	98.56
3.25	1.244	3.13	122.26
3.50	1.132	3.68	143.63
3.75	0.826	6.69	260.94
4.00	0.557	10.00	390.18
4.25	0.379	8.97	350.16
4.50	0.244	4.73	222.48
4.75	0.167	3.26	127.37
5.00	0.050	1.17	45.83
5.50	0.003	0.77	30.17
6.00	0.001	0.53	20.97

Table 16. Reduced data for run #8.

Packed bed height: 3.25 in.	Air velocity: 90 ft./min.	Particle size:	100% 40 mesh, 0% 80 mesh.
H inches	$\bar{\rho}$ g./cc.	ISU	χ^2_{39}
1.00	1.157	6.67	260.28
1.50	1.111	7.25	282.82
2.00	1.071	3.32	129.73
2.50	1.084	4.60	179.64
3.00	1.091	4.35	169.93
3.50	0.954	5.64	220.24
4.00	0.698	4.79	187.10
4.50	0.502	6.12	238.70
5.00	0.327	4.36	170.34
5.50	0.199	4.79	186.94
6.00	0.134	4.04	157.68
6.50	0.091	1.51	59.06
7.00	0.070	1.29	50.57

Table 17. Reduced data for run #9.

Packed bed height: 6.20 in.	Air velocity: 30 ft./min.	Particle size:	0% 40 mesh. 100% 80 mesh.
H inches	$\bar{\rho}$ g./cc.	ISU	χ^2_{39}
1.00	1.216	3.42	133.49
1.50	1.204	3.11	121.66
2.00	1.229	5.24	204.41
2.50	1.187	4.66	181.96
3.00	1.189	7.68	299.79
3.50	1.171	9.95	388.10
4.00	1.151	7.94	309.67
4.50	1.162	6.58	256.92
5.00	1.141	6.77	264.29
5.50	1.154	8.17	318.65
6.00	1.177	8.22	320.68
6.50	1.139	6.32	246.68
6.75	1.110	10.00	390.17
7.00	1.005	11.37	443.81
7.25	0.871	14.75	575.55
7.50	0.715	9.90	386.22
7.75	0.548	19.34	754.32
8.00	0.412	21.06	821.61
8.25	0.310	14.42	562.41
8.50	0.208	12.44	485.52
8.75	0.138	7.60	296.53
9.00	0.086	3.99	155.93
9.50	0.041	3.13	122.28
10.00	0.026	1.12	44.05

Table 18. Reduced data for run # 10*.

Packed bed height: 6.20 in.	Air velocity: 60 ft./min.	Particle size:	0% 40 mesh, 100% 80 mesh.
H inches	$\bar{\rho}$ g./cc.	ISU	χ^2_{39}
1.00	1.058	5.43	212.12
1.50	1.060	5.98	233.60
2.00	0.949	8.18	319.03
2.50	0.945	11.33	441.98
3.00	0.915	5.36	209.40
4.00	0.899	10.65	415.50
5.00	0.930	10.19	397.62
5.50	0.908	13.47	525.57

Table 18. (concl.)

H inches	$\bar{\rho}$ g./cc.	ISU	χ^2_{39}
6.00	0.906	8.04	313.65
6.25	0.874	13.29	518.55
6.50	0.886	10.45	407.91
6.75	0.799	16.09	627.73
7.00	0.786	21.61	843.05
7.50	0.598	19.59	764.24
8.00	0.470	27.32	1065.48
8.50	0.360	19.78	771.65
9.00	0.247	30.60	1193.68
9.50	0.136	8.38	326.86
10.00	0.120	9.65	376.72
10.50	0.101	7.80	304.44
11.00	0.065	1.96	76.82
12.00	0.032	0.69	26.92
13.00	0.025	1.01	39.50

* Equipment drifted and calibration is slightly in error.

Table 19. Reduced data for run #11*.

Packed bed height: 6.20 in. Air velocity: 90 ft./min. Particle size: 0% 40 mesh, 100% 80 mesh.

H inches	$\bar{\rho}$ g./cc.	ISU	χ^2_{39}
1.00	0.990	6.14	827.56
1.50	1.002	5.07	601.75
2.00	1.012	7.76	657.95
2.50	0.924	7.28	419.14
3.00	0.961	8.05	705.38
3.50	0.948	10.67	460.15
4.00	0.973	8.87	259.97
4.50	1.030	12.87	433.12
5.00	1.007	10.52	464.07
5.50	1.039	18.12	246.36
6.00	0.981	7.32	170.20
6.50	0.901	12.11	286.50
7.00	0.788	15.67	159.86
7.25	0.739	18.84	103.84
7.50	0.662	17.45	239.60
7.75	0.578	21.21	197.87
8.00	0.555	15.42	302.76
8.25	0.488	16.87	284.19
8.50	0.407	10.74	313.99

Table 19. (concl.).

H inches	$\bar{\rho}$ g./cc.	ISU	χ^2_{39}
8.75	0.366	18.08	416.18
9.00	0.343	11.79	346.21
9.25	0.296	6.66	501.93
9.50	0.285	11.10	410.51
9.75	0.251	11.89	706.83
10.00	0.199	6.31	285.63
10.50	0.155	4.36	472.42
11.00	0.134	7.34	611.39
11.50	0.110	4.09	735.09
12.00	0.076	2.66	680.61
13.00	0.017	1.39	54.21

* Equipment drifted and calibration is slightly in error.

Table 20. Reduced data for run #12.

Packed bed height: 9.35 in. Air velocity: 30 ft./min. Particle size: 0% 40 mesh, 100% 80 mesh.

H inches	$\bar{\rho}$ g./cc.	ISU	χ^2_{39}
1.00	1.206	2.67	104.42
1.50	1.215	5.28	206.07
2.00	1.216	3.38	132.02
2.50	1.185	3.30	128.86
3.00	1.198	6.06	236.55
3.50	1.154	3.88	151.59
4.00	1.168	7.05	275.32
4.50	1.189	7.73	301.60
5.00	1.117	9.86	384.64
5.50	1.147	7.19	280.47
6.00	1.151	8.53	332.71
6.50	1.192	7.54	294.11
7.00	1.174	9.31	363.27
7.50	1.165	4.23	165.28
8.00	1.173	9.91	386.53
8.50	1.183	9.78	381.68
9.00	1.213	4.79	187.10
9.25	1.172	13.09	510.68
9.50	1.177	10.60	413.46
9.75	1.183	8.11	316.45
10.00	1.134	10.25	399.80

Table 20. (concl.).

H inches	$\bar{\rho}$ g./cc.	ISU	χ^2_{39}
10.50	1.049	8.83	344.75
11.00	0.926	11.48	448.09
11.50	0.671	22.28	869.29
12.00	0.371	28.99	1130.63
12.50	0.212	20.28	790.93
13.00	0.059	9.16	357.32
13.50	0.045	22.50	877.65

Table 21. Reduced data for run #13.

Packed bed height: 9.35 in. Air velocity: 60 ft./min. Particle size: 0% 40 mesh, 100% 80 mesh.

H inches	$\bar{\rho}$ g./cc.	ISU	χ^2_{39}
1.00	1.030	4.97	193.94
1.50	1.036	3.86	150.76
2.00	1.023	5.31	207.40
2.50	1.029	5.91	230.85
3.00	1.002	8.00	312.30
3.50	1.003	6.57	256.55
4.00	1.026	7.79	304.19
4.50	1.009	13.25	517.13
5.00	1.029	13.14	512.76
5.50	1.094	6.91	269.68
6.00	1.112	11.71	457.05
6.50	1.043	11.07	431.92
7.00	1.053	14.76	575.80
7.50	1.090	21.52	839.55
8.00	1.108	28.42	1108.67
8.50	1.092	21.16	825.37
9.00	1.097	18.85	735.50
9.25	1.069	15.92	621.03
9.50	1.005	22.42	874.59
10.00	0.995	9.50	370.81
10.50	0.967	10.96	427.48
11.00	0.826	18.15	707.99
11.50	0.731	14.09	549.55
12.00	0.617	23.58	919.87
12.50	0.601	29.78	1161.62
13.00	0.518	35.80	1396.35
13.25	0.412	43.00	1677.27

Table 21. (concl.).

H inches	$\bar{\rho}$ g./cc.	ISU	χ^2_{39}
13.50	0.382	28.79	1123.09
14.00	0.319	29.65	1156.43
14.50	0.279	50.28	1961.10
15.00	0.202	30.73	1198.48

Table 22. Reduced data for run #14.

Packed bed height: 3.25 in. Air velocity: 30 ft./min. Particle size: 0% 40 mesh, 100% 80 mesh.

H inches	$\bar{\rho}$ g/.cc.	ISU	χ^2_{39}
1.00	1.198	3.72	145.31
1.50	1.202	5.66	221.08
2.00	1.213	2.94	114.68
2.50	1.217	5.65	220.58
3.00	1.195	7.22	281.58
3.50	1.209	4.69	183.17
3.75	1.086	7.24	282.47
4.00	0.884	3.50	136.52
4.25	0.606	11.03	430.33
4.50	0.390	9.29	362.32
4.75	0.258	5.88	229.40
5.00	0.127	3.88	151.60
5.50	0.086	1.61	62.86
6.00	0.061	0.95	37.42

Table 23. Reduced data for run #15.

Packed bed height: 3.25 in. Air velocity: 60 ft./min. Particle size: 0% 40 mesh, 100% 80 mesh.

H inches	$\bar{\rho}$ g./cc.	ISU	χ^2_{39}
1.00	1.021	4.69	182.96
1.50	0.993	3.81	148.60
2.00	1.029	6.19	241.71
2.50	1.041	7.89	307.71

Table 23. Reduced data for run #15.

H inches	$\bar{\rho}$ g./cc.	ISU	χ^2_{39}
3.00	1.037	7.81	304.86
3.50	1.016	7.40	288.97
3.75	0.988	7.65	298.47
4.00	0.862	6.85	267.15
4.25	0.716	10.24	399.70
4.50	0.562	7.09	276.73
4.75	0.428	12.18	475.39
5.00	0.314	4.59	179.38
5.25	0.228	8.18	319.32
5.75	0.011	4.44	173.27
6.00	0.052	4.28	167.27
6.50	0.033	2.06	80.59
7.00	0.017	0.53	20.81

Table 24. Reduced data for run #16.

Packed bed height: 3.25 in.	Air velocity: 90 ft./min.	Particle size:	0% 40 mesh, 100% 80 mesh.
H inches	$\bar{\rho}$ g./cc.	ISU	χ^2_{39}
1.00	0,892	4.29	167.41
1.50	0.897	3.94	153.85
2.00	0.906	7.18	280.21
2.50	0.878	7.90	308.23
3.00	0.941	7.27	283.91
3.50	0.903	5.91	230.78
4.00	0.708	9.80	382.58
4.50	0.497	12.31	480.38
4.75	0.407	9.16	357.37
5.00	0.342	9.58	373.72
5.25	0.286	8.21	320.21
5.50	0.238	5.10	199.19
5.75	0.201	9.67	377.21
6.00	0.091	4.05	158.08
6.25	0.086	3.58	139.87
6.50	0.066	4.21	164.51
7.00	0.046	1.14	44.63
7.50	0.013	0.34	13.62
8.00	0.049	1.42	55.45

** Run #17 was a calibration check.

Table 25. Reduced data for run #18.

Packed bed height: 6.50 in.	Air velocity: 30 ft./min.	Particle size:	95% 40 mesh, 5% 80 mesh.
H inches	$\bar{\varrho}$ g./cc.	ISU	χ^2_{39}
1.00	1.305	1.20	47.07
1.50	1.310	2.04	79.86
2.00	1.303	2.30	89.73
2.50	1.299	2.46	96.18
3.00	1.335	2.01	78.63
3.50	1.346	3.61	140.81
4.00	1.339	2.90	113.33
4.50	1.330	2.60	101.59
5.00	1.337	4.56	177.96
5.50	1.312	4.52	176.32
6.00	1.330	4.33	168.97
6.25	1.338	5.93	231.55
6.50	1.323	5.20	203.14
6.75	1.348	6.23	243.08
7.00	1.294	2.83	110.51
7.25	1.135	3.76	146.97
7.75	0.956	7.85	306.22
8.00	0.403	12.11	472.38
8.50	0.189	1.68	65.86
9.00	0.147	0.74	28.93

Table 26. Reduced data for run #19.

Packed bed height: 6.50 in.	Air velocity: 60 ft./min.	Particle size:	95% 40 mesh, 5% 80 mesh.
H inches	$\bar{\varrho}$ g./cc.	ISU	χ^2_{39}
1.00	1.210	3.06	119.44
1.50	1.215	4.63	180.82
2.00	1.192	6.35	247.76
2.50	1.140	4.84	189.09
3.00	1.141	7.18	280.04
3.50	1.164	5.04	196.64
4.00	1.124	5.46	213.00
4.50	1.170	8.14	317.76
5.00	1.148	9.90	386.44
5.50	1.138	12.73	397.10
6.00	1.131	10.63	243.40
6.50	1.128	6.24	328.79

Table 26. (concl.).

H inches	$\bar{\rho}$ g./cc.	ISU	χ^2_{39}
7.00	1.051	8.43	496.51
7.25	1.016	10.18	414.63
7.50	0.944	6.63	258.68
7.75	0.811	9.34	364.55
8.00	0.710	11.54	450.08
8.25	0.669	18.09	705.61
8.50	0.553	25.53	995.83
8.75	0.485	19.07	744.00
9.00	0.414	15.39	600.52
9.50	0.307	16.80	655.36
10.50	0.078	31.80	124.31

Table 27. Reduced data for run #20.

Packed bed height: 6.50 in. Air velocity: 90 ft./min. Particle size: 95% 40 mesh, 5% 80 mesh.

H inches	$\bar{\rho}$ g./cc.	ISU	χ^2_{39}
1.00	1.096	2.20	86.13
1.50	1.092	4.83	188.65
2.00	1.078	4.02	156.93
2.50	1.058	6.08	237.14
3.00	1.049	5.56	216.87
3.50	1.055	6.36	248.31
4.00	1.048	8.78	342.54
4.50	1.023	9.01	351.70
5.00	1.047	9.71	378.80
5.50	1.059	12.33	480.87
6.00	1.023	10.57	412.52
6.50	1.013	13.32	519.61
7.00	0.925	8.98	350.59
7.50	0.773	12.10	472.06
7.75	0.699	13.61	530.91
8.00	0.655	11.49	448.35
8.25	0.615	12.83	500.74
8.50	0.564	16.04	625.78
8.75	0.510	9.91	386.60
9.00	0.489	24.01	936.77
9.25	0.460	15.32	597.80
9.50	0.419	14.11	550.43
10.00	0.350	21.04	820.56

Table 27. (concl.).

H inches	$\bar{\rho}$ g./cc.	ISU	χ^2_{39}
10.50	0.283	9.25	361.06
11.00	0.173	9.70	378.45
11.50	0.100	9.10	355.23
12.00	0.073	8.03	313.35
12.50	0.024	1.86	72.86

Table 28. Reduced data for run #21.

Packed bed height: 6.50 in. Air velocity: 30 ft./min. Particle size: 90% 40 mesh. 10% 80 mesh.

H inches	$\bar{\rho}$ g./cc.	ISU	χ^2_{39}
1.00	1.307	3.19	124.48
1.50	1.309	2.83	110.41
2.00	1.290	3.21	125.46
2.50	1.290	3.76	146.69
3.00	1.267	4.19	163.50
3.50	1.265	3.91	152.66
4.00	1.255	5.63	219.65
4.50	1.248	5.36	209.15
5.00	1.260	4.66	181.80
5.50	1.252	4.12	160.82
6.00	1.252	5.24	204.57
6.50	1.239	6.16	240.59
7.00	1.199	9.88	385.37
7.25	1.088	7.03	274.41
7.50	0.982	12.63	492.75
7.75	0.652	13.56	528.87
8.00	0.491	22.79	888.95
8.25	0.329	13.05	508.96
8.50	0.191	4.84	189.04
9.00	0.036	2.18	85.38

Table 29. Reduced data for run #22.

Packed bed height: 6.50 in.	Air velocity: 60 ft./min.	Particle size:	90% 40 mesh, 10% 80 mesh.
H inches	$\bar{\rho}$ g./cc.	ISU	χ^2_{39}
1.00	1.196	3.16	123.46
1.50	1.146	3.48	135.80
2.00	1.159	5.24	204.73
2.50	1.140	8.03	313.36
3.00	1.115	5.98	233.51
3.50	1.095	5.64	219.99
4.00	1.084	11.78	459.56
4.50	1.084	6.54	255.10
5.00	1.114	8.05	314.33
5.50	1.108	8.01	312.63
6.00	1.081	13.71	534.89
6.50	1.083	10.31	402.21
7.00	1.008	9.99	389.77
7.50	0.908	9.54	372.15
7.75	0.710	10.15	396.07
8.00	0.651	15.66	611.03
8.25	0.625	19.26	751.49
8.50	0.516	18.43	719.11
8.75	0.486	29.50	1150.81
9.00	0.399	21.51	838.94
9.25	0.346	12.33	480.94
9.50	0.240	10.93	426.34
10.00	0.146	6.08	237.50
10.50	0.037	3.30	128.79
11.00	0.028	1.22	47.91

Table 30. Reduced data for run #23.

Packed bed height: 6.50 in.	Air velocity: 90 ft./min.	Particle size:	90% 40 mesh, 10% 80 mesh.
H inches	$\bar{\rho}$ g./cc.	ISU	χ^2_{39}
1.00	1.065	2.05	80.16
1.50	1.079	3.95	154.27
2.00	1.043	3.83	149.61
3.00	0.947	5.11	199.66
3.50	0.893	4.74	184.97
4.00	0.843	15.44	602.21
4.50	0.808	15.74	613.93

Table 30. (concl.).

H inches	$\bar{\rho}$ g./cc.	ISU	χ^2_{39}
5.00	0.847	13.48	525.75
5.50	0.813	14.64	571.32
6.00	0.799	13.13	512.15
6.50	0.821	19.86	774.63
7.00	0.717	16.11	628.55
7.50	0.573	7.31	285.17
7.75	0.586	16.93	660.51
8.00	0.520	10.73	418.62
8.25	0.465	10.31	402.41
8.50	0.447	19.11	745.37
8.75	0.400	15.01	585.72
9.00	0.346	11.45	446.56
9.25	0.293	14.50	565.55
9.50	0.260	15.93	621.54
10.00	0.220	15.19	592.49
10.50	0.094	10.73	418.50
11.50	0.039	5.91	230.82

Table 31. Reduced data for run #24.

Packed bed height: 6.50 in. Air velocity; 30 ft./min. Particle size: 2% 40 mesh, 98% 80 mesh.

H inches	$\bar{\rho}$ g./cc.	ISU	χ^2_{39}
1.00	1.205	2.99	116.72
1.50	1.206	3.23	126.16
2.00	1.183	3.44	134.31
2.50	1.187	4.08	159.28
3.00	1.133	5.33	208.21
3.50	1.138	7.18	280.26
4.00	1.095	5.11	199.56
4.50	1.108	5.98	233.60
5.00	1.101	7.57	295.27
5.50	1.133	5.07	197.83
6.00	1.129	7.53	294.00
6.50	1.102	8.34	325.47
7.00	1.112	10.89	425.00
7.25	1.044	5.15	200.86
7.50	0.978	10.70	417.57
7.75	0.783	5.71	222.96
8.00	0.656	21.37	833.43

Table 31. (concl.).

H inches	$\bar{\rho}$ g./cc.	ISU	χ^2_{39}
8.25	0.501	14.39	561.56
8.50	0.423	17.04	664.67
8.75	0.299	13.70	534.53
9.00	0.215	14.27	556.64

Table 32. Reduced data for run #25.

Packed bed height: 6.50 in.	Air velocity: 60 ft./min.	Particle size:	2% 40 mesh, 98% 80 mesh.
H inches	$\bar{\rho}$ g./cc.	ISU	χ^2_{39}
1.00	1.090	2.85	111.44
1.50	1.069	3.93	153.63
2.00	1.071	5.51	214.89
2.50	1.081	5.40	210.71
3.00	1.032	8.24	321.65
3.50	1.007	10.74	418.97
4.00	1.039	7.70	300.59
4.50	1.016	8.52	332.44
5.00	1.027	10.95	427.22
5.50	1.025	10.83	422.47
6.00	1.053	9.94	387.72
6.50	1.032	10.85	423.31
7.00	0.980	10.25	399.94
7.50	0.841	14.95	583.18
7.75	0.758	11.54	450.39
8.00	0.614	18.74	731.16
8.25	0.586	26.97	1052.01
8.50	0.500	13.10	511.13
8.75	0.454	23.38	911.97
9.00	0.399	19.42	757.50
9.25	0.324	22.34	871.40
9.50	0.259	9.52	371.30
10.00	0.221	16.20	632.08
10.50	0.132	5.62	219.48
11.50	0.015	3.95	154.39
12.00	0.017	1.85	72.27

Table 33. Reduced data for run #26.

Packed bed height: 6.50 in. Air velocity: 90 ft./min. Particle size: 2% 40 mesh, 98% 80 mesh.

H inches	$\bar{\rho}$ g./cc.	ISU	χ^2_{39}
1.00	0.948	3.72	145.22
1.50	0.944	3.53	137.75
2.00	0.929	6.02	234.81
2.50	0.958	5.67	221.16
3.00	0.934	12.67	494.29
3.50	0.974	13.27	517.65
4.00	0.967	11.95	466.16
4.50	1.012	11.52	449.64
5.00	1.012	7.57	295.51
5.50	0.985	9.17	357.82
6.00	1.027	7.99	311.68
6.50	1.004	8.68	338.68
7.00	0.938	8.00	312.36
7.50	0.741	14.41	562.17
7.75	0.649	13.65	532.65
8.00	0.630	12.82	500.13
8.25	0.535	10.57	412.48
8.50	0.471	11.15	435.09
8.75	0.435	20.29	791.41
9.00	0.380	12.30	479.78
9.25	0.359	20.87	814.12
9.50	0.316	10.87	424.29
9.75	0.290	23.68	923.70
10.00	0.234	6.64	259.17
10.50	0.213	9.70	378.52
11.00	0.184	10.38	405.06
11.50	0.099	7.52	293.62
12.00	0.072	3.32	129.57
12.50	0.053	2.60	101.68
13.00	0.040	1.71	66.77

Table 34. Reduced data for run #27.

Packed bed height: 6.50 in. Air velocity: 30 ft./min. Particle size: 5% 40 mesh, 95% 80 mesh.

H inches	$\bar{\rho}$ g./cc.	ISU	χ^2_{39}
1.00	1.202	3.50	136.85
1.50	1.212	3.37	131.78
2.00	1.234	3.43	133.89
2.50	1.178	5.07	198.03
3.00	1.179	5.56	217.02
3.50	1.159	3.68	143.73

Table 34. (concl.).

H inches	$\bar{\rho}$ g./cc.	ISU	χ^2_{39}
4.50	1.145	7.04	274.68
5.00	1.132	4.82	188.12
5.50	1.146	8.63	336.83
6.00	1.155	7.98	311.50
6.25	1.166	7.58	295.62
6.50	1.160	9.73	379.60
6.75	1.159	8.17	318.97
7.00	1.139	8.90	347.44
7.50	1.025	8.56	333.90
8.00	0.726	16.20	632.09
8.50	0.414	16.75	653.46
9.00	0.270	12.45	485.71
9.50	0.095	4.39	171.37
10.00	0.042	2.83	110.42
11.00	0.004	0.98	38.39

Table 35. Reduced data for run #28.

Packed bed height: 6.50 in.	Air velocity: 60 ft./min.	Particle size:	5% 40 mesh, 95% 80 mesh.
H inches	**$\bar{\rho}$ g./cc.**	**ISU**	**χ^2_{39}**
1.00	1.081	4.50	175.71
1.50	1.072	3.62	141.39
2.00	1.054	4.82	188.19
2.50	1.042	5.10	199.23
4.00	1.042	6.88	268.42
5.00	1.061	7.75	302.48
5.50	1.079	9.99	389.91
6.00	1.064	9.04	352.92
6.25	1.060	6.96	271.61
6.50	1.080	15.17	591.96
6.75	1.040	9.86	384.57
7.00	1.013	8.39	327.33
7.50	0.946	13.39	522.29
8.00	0.721	13.26	517.39
8.50	0.571	21.01	819.52
9.00	0.440	12.61	491.99
10.00	0.256	16.82	656.01
10.50	0.183	3.62	141.35
11.00	0.070	9.51	371.01
11.50	0.039	2.76	107.72
12.00	0.004	1.75	68.54

Table 36. Reduced data for run #29.

Packed bed height: 6.50 in.	Air velocity: 90 ft./min.	Particle size:	5% 40 mesh, 95% 80 mesh.
H inches	$\bar{\rho}$ g./cc.	ISU	χ^2_{39}
1.00	0.953	2.50	97.61
1.50	0.963	3.29	128.67
2.00	0.965	5.43	211.77
2.50	0.976	10.35	403.80
3.00	0.974	4.54	177.18
3.50	0.952	4.75	185.59
4.00	1.001	9.34	364.55
4.50	1.005	11.16	435.24
5.00	1.014	12.77	498.34
5.50	1.023	12.06	470.70
6.00	1.025	11.68	455.69
6.50	0.968	9.66	388.76
7.00	0.926	11.58	451.88
7.50	0.715	14.46	564.07
7.75	0.656	10.34	403.31
8.00	0.587	9.31	363.28
8.25	0.555	14.79	576.86
8.50	0.460	17.46	681.27
8.75	0.416	14.65	571.38
9.00	0.398	14.24	555.57
9.25	0.342	18.53	722.74
9.50	0.374	13.56	529.09
10.00	0.236	6.36	248.11
10.50	0.184	5.40	210.89
11.00	0.111	5.94	231.68
11.50	0.088	3.00	117.00
12.00	0.070	4.27	166.76
12.50	0.045	2.45	95.87
13.00	0.035	1.43	55.93

Table 37. Reduced data for run #30.

Packed bed height: 6.15 in.	Air velocity: 30 ft./min.	Particle size:	50% 40 mesh, 50% 80 mesh.
H inches	$\bar{\rho}$ g./cc.	ISU	χ^2_{39}
1.00	1.243	2.67	104.13
1.50	1.261	3.47	135.53
2.00	1.249	5.48	213.88
2.50	1.247	3.18	124.26
3.00	1.238	5.44	212.51

Table 37. (concl.).

H inches	$\bar{\rho}$ g./cc.	ISU	χ^2_{39}
3.50	1.218	8.03	313.29
4.00	1.202	7.01	273.73
4.50	1.171	11.13	434.11
5.00	1.193	9.34	364.48
5.50	1.194	7.48	291.86
6.00	1.211	7.28	283.96
6.50	1.194	9.49	370.47
6.75	1.131	9.91	386.52
7.00	1.045	11.42	445.51
7.25	0.911	8.03	313.41
7.50	0.656	16.34	637.51
7.75	0.482	25.49	994.11
8.00	0.367	33.20	1295.13
8.25	0.223	12.05	469.98
8.50	0.116	7.41	289.09
9.00	0.033	2.44	95.20

Table 38. Reduced data for run #31.

Packed bed height: 6.15 in. Air velocity: 60 ft./min. Particle size: 50% 40 mesh, 50% 80 mesh.

H inches	$\bar{\rho}$ g./cc.	ISU	χ^2_{39}
1.00	1.146	4.64	180.98
1.50	1.170	5.14	200.65
2.00	1.151	4.94	192.78
2.50	1.155	8.34	325.27
3.00	1.124	9.61	374.79
3.50	1.098	10.69	417.21
4.00	1.113	12.08	471.45
4.50	1.130	8.06	314.67
5.00	1.135	13.40	522.60
5.50	1.159	10.29	401.36
6.00	1.135	11.51	448.93
6.50	1.093	11.97	466.93
7.00	0.976	11.69	456.04
7.25	0.847	18.71	729.93
7.50	0.750	15.04	586.67
7.75	0.659	15.20	593.06
8.00	0.591	26.23	1022.97
8.25	0.478	16.71	652.04

Table 38. (concl.).

H inches	$\bar{\rho}$ g./cc.	ISU	χ^2_{39}
8.50	0.385	23.92	933.21
8.75	0.325	14.31	558.14
9.00	0.278	11.81	460.86
9.50	0.190	17.63	687.81
10.00	0.089	9.86	384.66
10.50	0.031	4.23	165.17
11.00	0.007	2.78	108.44

Table 39. Reduced data for run #32.

Packed bed height: 6.10 in. Air velocity: 90 ft./min. Particle size: 50% 40 mesh, 50% 80 mesh.

H inches	$\bar{\rho}$ g./cc.	ISU	χ^2_{39}
1.00	1.033	4.76	186.01
1.50	1.037	5.47	213.70
2.00	1.043	8.34	325.36
2.50	1.045	5.70	222.60
3.00	1.014	9.74	379.97
3.50	1.046	13.88	541.33
4.00	1.067	11.69	456.20
4.50	1.098	12.19	475.62
5.00	1.071	16.23	633.15
5.50	1.096	18.60	725.51
6.00	1.050	29.98	1169.52
6.50	1.029	12.96	505.44
7.00	0.947	19.21	749.24
7.25	0.849	10.87	424.17
7.50	0.747	17.53	683.88
7.75	0.691	16.66	649.85
8.00	0.605	19.58	763.85
8.25	0.587	25.00	975.31
8.50	0.492	20.90	815.35
8.75	0.458	17.67	689.37
9.00	0.373	17.63	687.81
9.25	0.343	16.98	662.53
9.50	0.324	19.01	741.75
10.00	0.228	13.69	533.94
10.50	0.141	7.32	285.85
11.00	0.091	8.09	315.62
11.50	0.064	4.43	188.43

Table 39. (concl.).

H inches	$\bar{\bar{\rho}}$ g./cc.	ISU	χ^2_{39}
12.00	0.057	4.80	187.45
12.50	0.034	1.71	66.75
13.00	0.017	2.81	109.65

Table 40. Reduced data for run #33.

Packed bed height: 6.50 in.	Air velocity: 30 ft./min.	Particle size:	10% 40 mesh, 90% 80 mesh.
H inches	**$\bar{\bar{\rho}}$ g./cc.**	**ISU**	**χ^2_{39}**
1.00	1.252	2.96	115.56
1.50	1.245	2.06	80.71
2.00	1.231	3.35	131.00
2.50	1.213	5.38	210.09
3.00	1.201	6.30	245.72
4.00	1.178	7.35	286.92
5.00	1.150	6.26	244.43
5.50	1.172	10.05	392.33
6.00	1.186	8.71	339.89
6.25	1.182	8.95	349.25
6.50	1.176	10.23	399.24
6.75	1.156	7.91	308.54
7.00	1.101	5.40	210.76
7.50	0.954	11.72	457.42
8.00	0.661	20.10	783.98
8.50	0.429	4.16	721.69
9.00	0.205	14.39	561.50
9.50	0.108	25.74	162.50
10.50	0.032	1.75	68.35

Table 41. Reduced data for run #34.

Packed bed height: 6.50 in.	Air velocity: 60 ft./min.	Particle size:	10% 40 mesh, 90% 80 mesh.
H inches	$\bar{\rho}$ g./cc.	ISU	χ^2_{39}
1.00	1.064	3.20	125.02
1.50	1.069	4.50	175.68
2.00	1.068	7.33	285.99
3.00	1.064	7.31	285.11
4.00	1.070	9.77	381.14
5.00	1.074	12.16	474.44
5.50	1.108	11.50	448.69
6.00	1.086	9.10	354.99
6.25	1.074	8.36	326.14
6.50	1.078	12.75	497.47
6.75	1.032	10.86	423.58
7.00	1.032	15.03	586.46
7.50	0.792	15.74	614.15
8.00	0.668	11.11	433.54
8.50	0.556	17.96	700.49
9.00	0.442	12.27	478.64
9.50	0.346	19.75	770.55
10.00	0.260	9.13	356.18
10.50	0.148	59,08	382.60
11.00	0.141	4.84	188.93
12.00	0.060	1.72	67.33
13.00	0.022	0.71	27.71

Table 42. Reduced data for run #35.

Packed bed height: 6.50 in.	Air velocity: 90 ft./min.	Particle size:	10% 40 mesh, 90% 80 mesh.
H inches	$\bar{\rho}$ g./cc.	ISU	χ^2_{39}
1.00	0.992	3.56	139.01
1.50	0.968	7.34	286.58
2.00	0.983	4.71	183.73
3.00	1.000	10.28	401.06
4.00	1.006	9.74	379.86
4.50	0.994	8.81	343.77
5.00	1.001	15.43	601.96
5.50	0.994	14.79	576.96
6.00	0.967	10.14	395.66
6.25	0.977	7.27	283.89

Table 42. (concl.).

H inches	$\bar{\rho}$ g./cc.	ISU	χ^2_{39}
6.50	0.976	9.80	382.58
6.75	0.909	9.42	367.66
7.00	0.794	14.98	584.46
7.50	0.717	16.96	661.59
8.00	0.610	13.65	532.66
9.00	0.438	10.23	399.05
10.00	0.292	14.60	569.73
10.50	0.248	6.49	253.38
11.00	0.207	10.41	406.05
12.00	0.115	3.49	136.24
13.00	0.082	8.58	334.71
14.00	0.057	0.67	26.49
15.00	0.032	1.28	50.30

Table 43. Reduced data for run #36'.

Packed bed height: 6.50 in.	Air velocity: 30 ft./min.	Particle size:	98% 40 mesh, 2% 80 mesh.
H inches	$\bar{\rho}$ g./cc.	ISU	χ^2_{39}
1.00	1.341	1.47	57.50
1.50	1.328	0.94	36.83
2.00	1.319	1.85	72.30
2.50	1.317	1.69	65.97
3.00	1.328	2.17	84.63
3.50	1.324	3.06	119.63
4.00	1.296	4.03	157.28
4.50	1.315	3.57	139.35
5.00	1.309	4.49	175.43
5.50	1.328	5.51	215.25
6.00	1.271	5.13	200.20
6.25	1.286	4.23	165.32
6.50	1.269	5.67	218.98
6.75	1.275	5.57	217.38
7.00	1.228	6.17	240.74
7.50	0.820	19.99	779.61
8.00	0.275	18.34	715.52
8.50	0.095	8.84	344.97
9.00	0.007	0.95	37.13

Table 44. Reduced data for run #37.

Packed bed height: 6.50 in.	Air velocity: 60 ft./min.	Particle size:	98% 40 mesh, 2% 80 mesh.
H inches	$\bar{\rho}$ g./cc.	ISU	χ^2_{39}
1.00	1.243	2.90	113.34
1.50	1.235	1.87	73.05
2.00	1.214	3.83	149.54
3.00	1.173	6.62	258.51
4.00	1.164	11.28	440.23
4.50	1.179	14.03	547.50
5.00	1.144	11.57	451.23
5.50	1.178	10.93	426.31
6.00	1.131	9.88	345.63
6.25	1.139	11.91	464.83
6.50	1.150	11.12	433.94
6.75	1.079	6.48	252.81
7.00	1.058	9.13	356.31
7.50	0.964	17.52	683.32
8.00	0.719	14.40	561.76
8.50	0.603	17.85	696.28
9.00	0.470	25.63	999.92
9.50	0.294	18.87	735.93
10.00	0.166	15.37	599.70
11.00	0.042	1.86	72.70

Table 45. Reduced data for run #38.

Packed bed height: 6.50 in.	Air velocity: 90 ft./min.	Particle size:	98% 40 mesh, 2% 80 mesh.
H inches	$\bar{\rho}$ g./cc.	ISU	χ^2_{39}
1.00	1.121	5.17	201.97
1.50	1.132	5.87	229.16
2.00	1.107	9.44	368.22
2.50	1.078	5.98	233.60
3.00	1.046	8.12	317.00
3.50	1.083	11.24	438.48
4.00	1.099	11.99	467.62
4.50	1.050	14.22	554.76
5.00	1.079	24.21	944.32
5.50	1.022	12.49	487.13
6.00	0.999	22.53	879.05
6.50	0.981	13.40	522.86
7.00	0.879	14.48	565.09

Table 45. (concl.).

H inches	$\bar{\rho}$ g./cc.	ISU	χ^2_{39}
7.50	0.767	17.98	701.30
7.75	0.750	20.63	804.69
8.00	0.675	10.32	402.84
8.25	0.603	12.62	492.26
8.50	0.589	17.95	700.09
8.75	0.542	14.50	565.52
9.00	0.504	16.01	624.48
9.25	0.511	46.82	1826.24
9.50	0.448	21.95	856.13
9.75	0.391	16.69	651.19
10.00	0.359	29.29	1142.48
10.50	0.294	20.40	795.87
11.00	0.235	22.49	877.17
11.50	0.178	32.07	1251.10
12.00	0.119	20.22	788.81
12.50	0.041	6.86	267.92
13.00	0.008	1.94	75.67

DYNAMIC CHARACTERISTICS OF GAS-SOLIDS FLUIDIZED BEDS USING RADIOACTIVE ISOTOPE TECHNIQUES

by

JOE JACKSON STEWART

B. S., Purdue University, 1959

AN ABSTRACT OF A THESIS

submitted in partial fulfillment of the

requirements for the degree

MASTER OF SCIENCE

Department of Nuclear Engineering

KANSAS STATE UNIVERSITY
OF AGRICULTURE AND APPLIED SCIENCE

1961

A radiation attenuation method was used to determine density fluctuations in gas-solids fluidized beds. A beam of gamma-radiation was directed through the fluidizing column, and density fluctuations were determined by detecting, measuring, and recording the portion of γ-radiation which was not attenuated by the fluidized bed.

A statistical approach to the study of bed quality was used. Data were subjected to a χ^2 test for goodness of fit, and an index of stability and uniformity (ISU) was defined as the ratio of the variance in the density of the fluidized bed to the variance in density of a packed bed with the same average density as the fluidized bed.

Vertical profiles of the average density and ISU were used to investigate the effect of the following operational variables upon bed quality: gas velocity, height in bed, i. e., the height above the distributor, packed bed height, particle size and bed composition. A detailed discussion of the effect of these variables is given.

It was found that gas velocity and height in bed had a more pronounced effect upon bed stability and uniformity than did the packed bed height, particle size, and bed composition. Better bed quality was characteristic of shallow beds and low gas velocity. The stability of the fluidized bed was found to decrease with increasing height above the distributor, indicating that bubbles grow as they move up the column. The point at which the bubbles break the dense-phase surface, i. e., the fluidized bed height, was characterized by a peak in the ISU profiles. This point was satisfactorily correlated with the inflection point of the vertical portion of the average density profile, and thus a precise measurement of bed expansion could be made. At low gas velocities, coarse particles produced better bed stability and uniformity than fine particles; however, this trend appeared to reverse as the gas velocity was increased. Channeling became prevalent at high velocities.

The IBM-650 computer was used in the statistical analysis of data, and a complete description of the program is given.